Most flows are unstable...

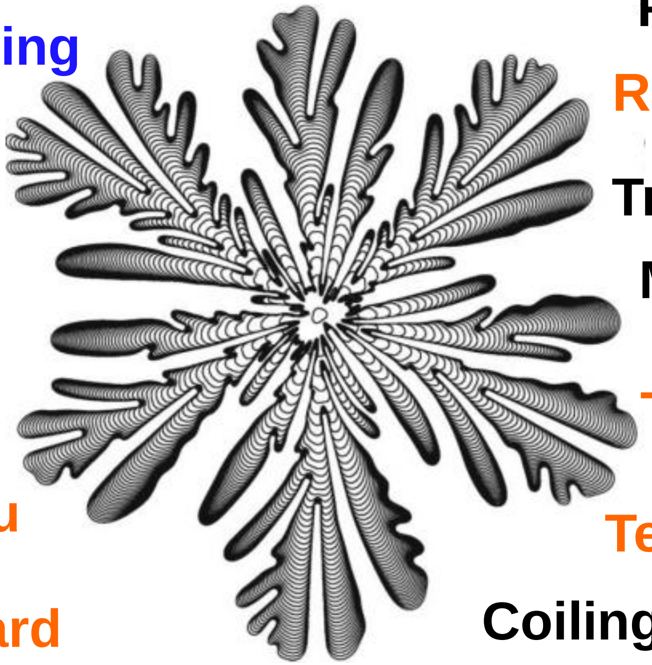

Vortex shedding

Saffman-Taylor

Flow separation

Tollmien-Schlichting

Rayleigh-Taylor

Lift-up and Streaks

Traffic waves

Meandering instability

Gravito-capillary waves

Taylor-Couette

Rayleigh-Plateau

Tearing instability

Rayleigh-Benard

Coiling instability

Benard-Marangoni

Kelvin-Helmholtz

SPATIALLY DEVELOPING SHEAR FLOWS

Flat plate boundary layer

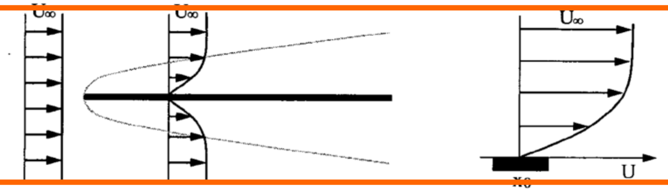

Mixing layer

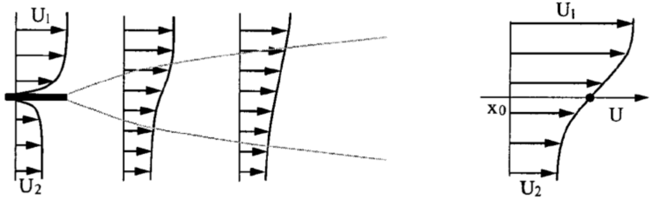

Cylinder wake

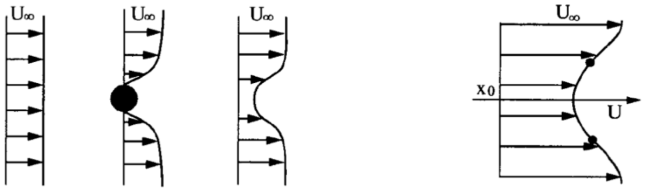

Plane channel flow

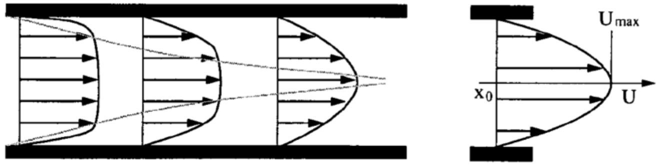

2D jet

PARALLEL FLOW CONCEPTS

Viscous 3D instabilities

3D Navier - Stokes equations

$$\nabla \cdot \mathbf{U} = 0\,,$$

$$\frac{\partial \mathbf{U}}{\partial t} + (\mathbf{U} \cdot \nabla)\mathbf{U} = -\,\nabla P + \frac{1}{\mathrm{Re}}\nabla^2 \mathbf{U}$$

Basic flow + perturbation

$$\mathbf{U}(\mathbf{x}, t) = U(y)\mathbf{e}_x + \mathbf{u}(\mathbf{x}, t)$$

$$P(\mathbf{x}, t) = P_0(x) + p(\mathbf{x}, t)$$

Basic flow

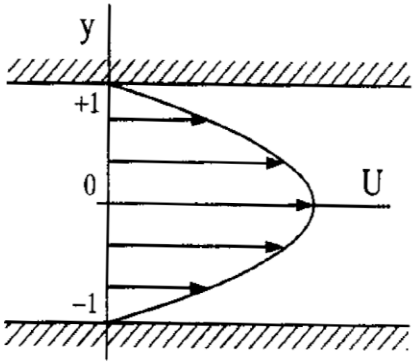

PARALLEL FLOW CONCEPTS

Viscous 3D instabilities

Squire's transformation

$$\tilde{k}^2 = k_x^2 + k_z^2 \,, \qquad \tilde{c} = c \,,$$

$$\tilde{k}\tilde{u} = k_x \hat{u} + k_z \hat{w} \,, \qquad \tilde{v} = \hat{v} \,, \qquad \tilde{p}/\tilde{k} = \hat{p}/k_x \,.$$

$$\tilde{k}\widetilde{\mathrm{Re}} = k_x \,\mathrm{Re}$$

3D dispersion relation

$$D(\mathbf{k}, \omega; \mathrm{Re}) \equiv \tilde{D}\left[(k_x^2 + k_z^2)^{1/2}, \frac{(k_x^2 + k_z^2)^{1/2}}{k_x}\omega; \frac{k_x}{(k_x^2 + k_z^2)^{1/2}}\mathrm{Re}\right] = 0$$

To each oblique mode $(\mathbf{k}, \omega)$ of temporal growth rate ω_i, at Reynolds number Re, corresponds a two-dimensional mode $(\tilde{k}, \tilde{\omega})$ of larger growth rate $\tilde{\omega}_i = \omega_i \sqrt{k_x^2 + k_z^2}/k_x$, at a *lower* Reynolds number $\widetilde{\mathrm{Re}} = \mathrm{Re}\, k_x/\sqrt{k_x^2 + k_z^2}$.

2D PARALLEL FLOW CONCEPTS

Dispersion relation

2D vorticity equation

$$\left(\frac{\partial}{\partial t}+\frac{\partial\Psi}{\partial y}\frac{\partial}{\partial x}-\frac{\partial\Psi}{\partial x}\frac{\partial}{\partial y}\right)\nabla^2\Psi=\frac{1}{Re}\nabla^4\Psi$$

Basic flow + perturbation

$$\Psi(x,t)=\int U(y)dy+\psi(x,y,t)$$

Linear vorticity equation

$$\left(\frac{\partial}{\partial t}+U(y)\frac{\partial}{\partial x}\right)\nabla^2\psi-U''(y)\frac{\partial\psi}{\partial x}=\frac{1}{Re}\nabla^4\psi$$

2D PARALLEL FLOW CONCEPTS

Dispersion relation

Normal mode decomposition

$$\psi(x,y,t) = \mathcal{R}e\left\{\phi(y)\, e^{i(kx-\omega t)}\right\}$$

Orr-Sommerfeld equation

$$[U(y)-c][\phi'' - k^2\phi] - U''(y)\,\phi = \frac{1}{i\,k\,Re}\left(\frac{d^2}{dy^2} - k^2\right)^2 \phi$$

$\phi(y)$ ⇨0 at $y = \pm\infty$

Dispersion relation

$$D(k,\omega;Re) = 0$$

Viscosity has limited stabilizing influence on K-H instability

$$Re := \Delta U \, \delta / \nu$$

$$\omega_{i,max} \frac{\delta}{\Delta U} \approx \sqrt{\frac{0,2}{1 + \underset{\text{constant}}{\textcircled{a}} / 0,2 Re}}$$

Viscosity has stabilizing influence on K-H instability

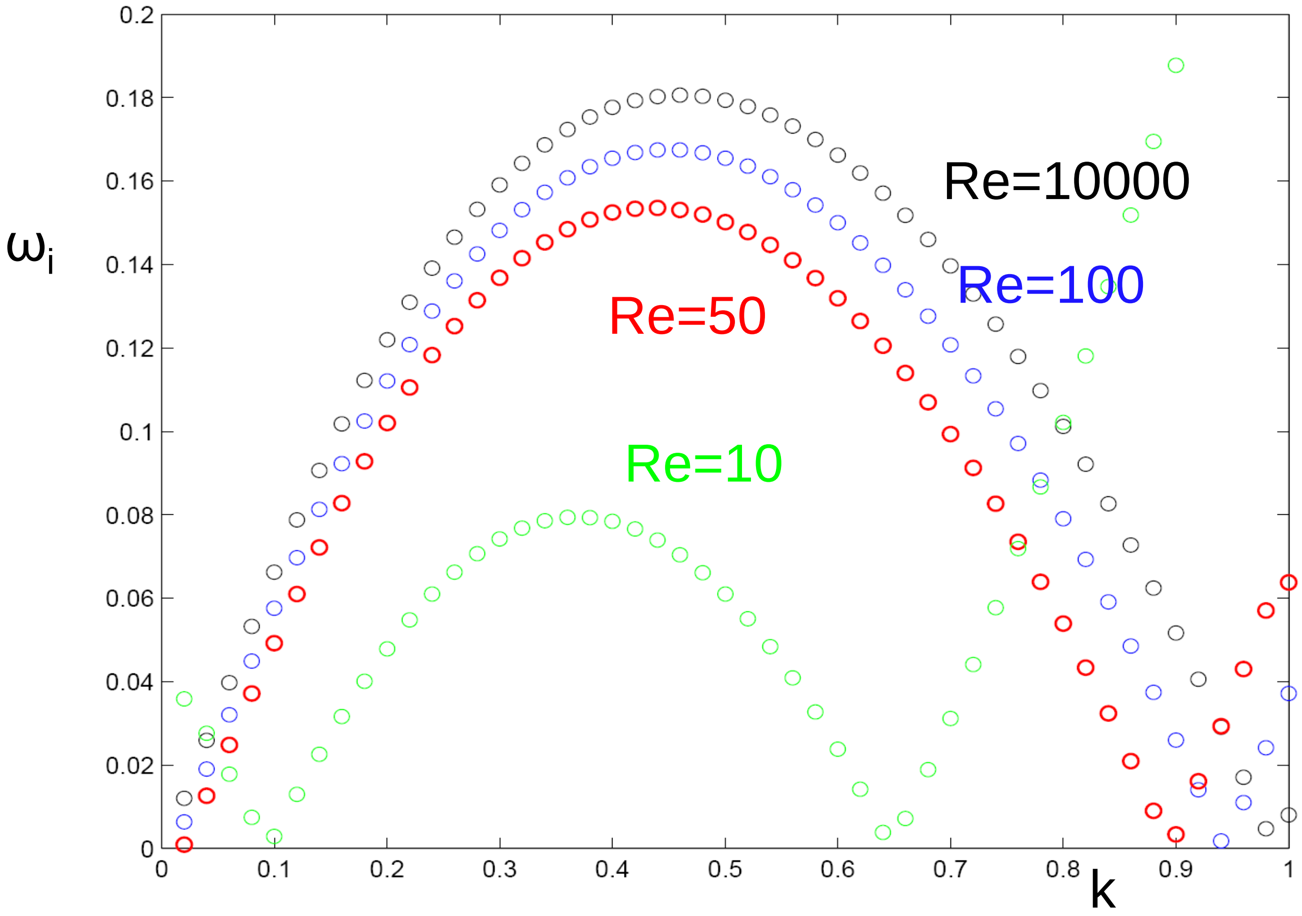

PARALLEL FLOW CONCEPTS

Viscous instabilities

Hyperbolic tangent mixing layer

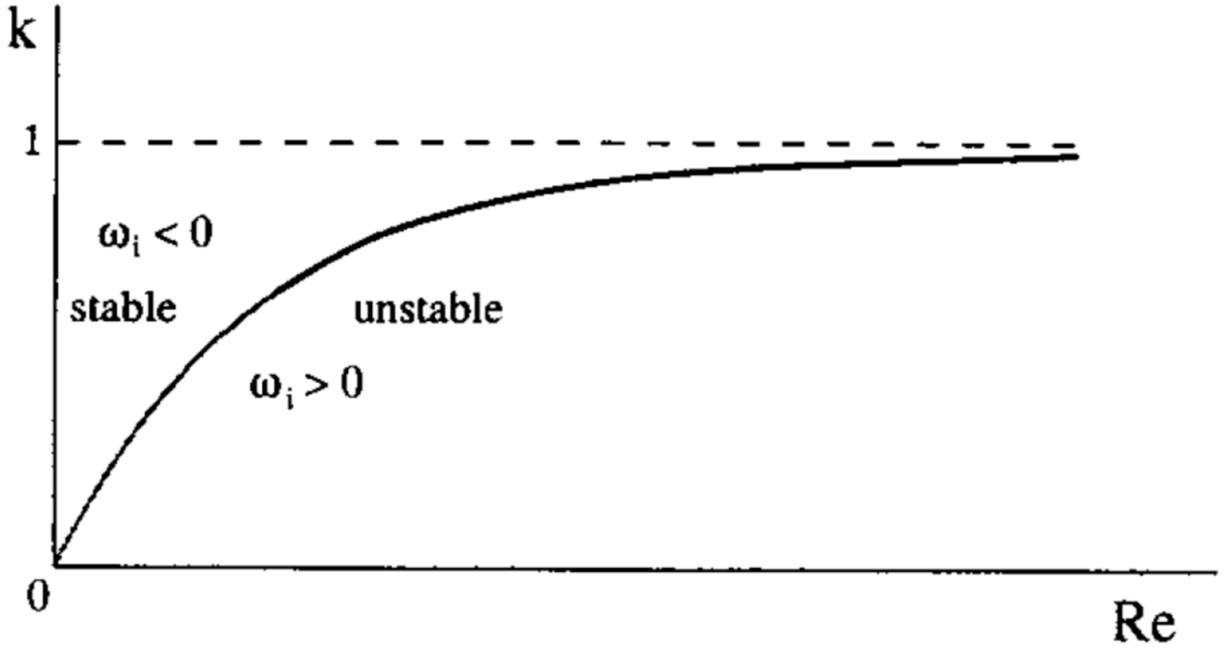

SPATIALLY DEVELOPING SHEAR FLOWS

Flat plate boundary layer

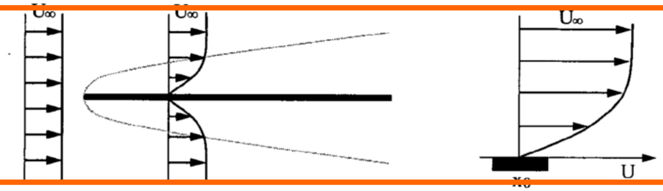

Mixing layer

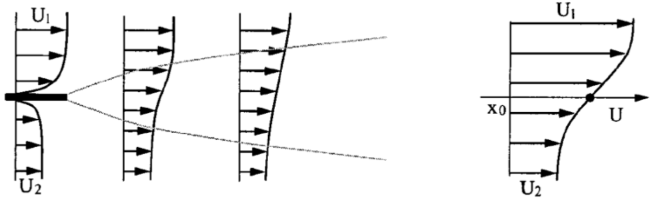

Cylinder wake

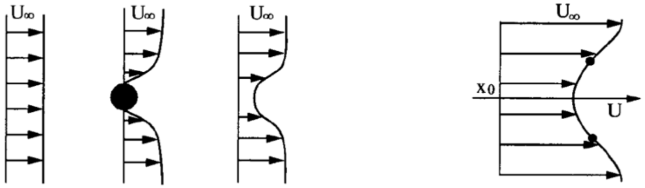

Plane channel flow

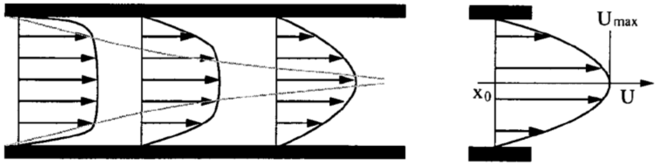

2D jet

What about stable flows (no inflexion point)?

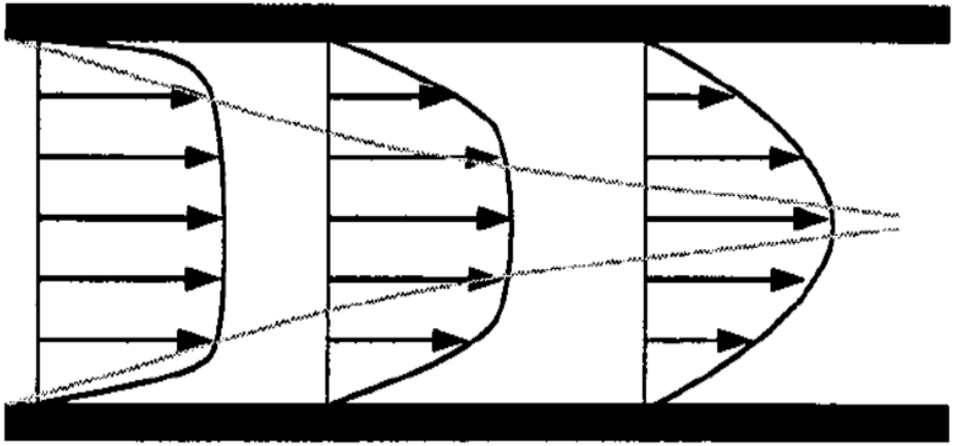

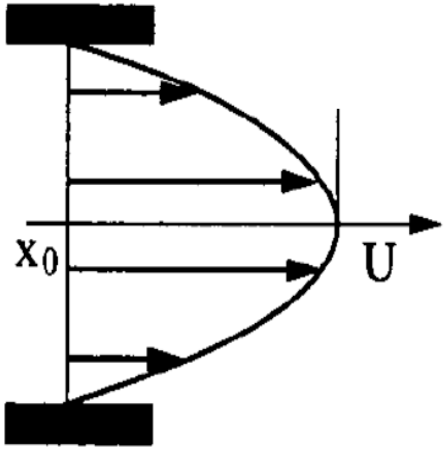

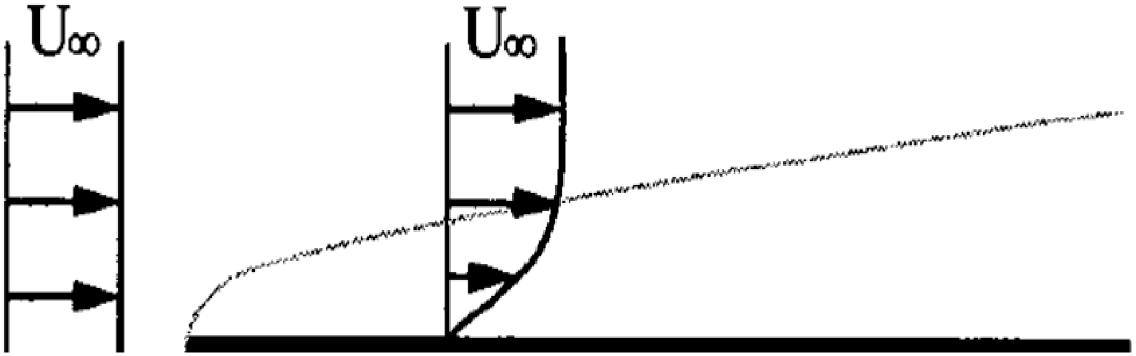

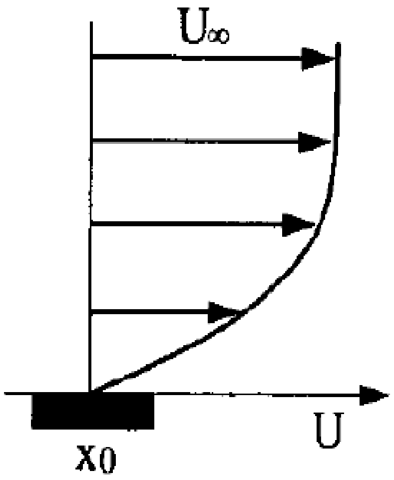

Plane poiseuille flow

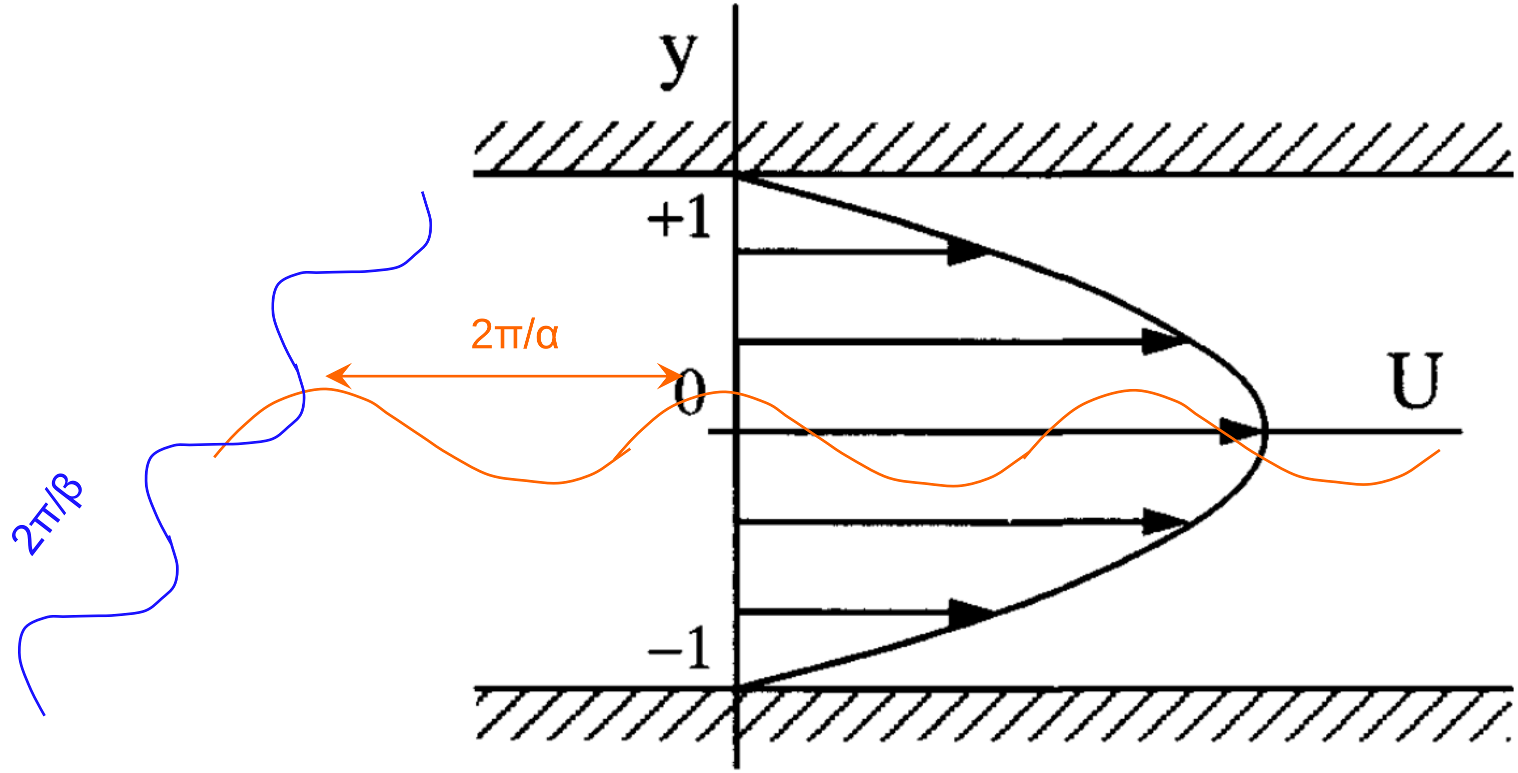

Plane poiseuille flow; Re=10000; α=1, β=0

No inflection point but unstable!

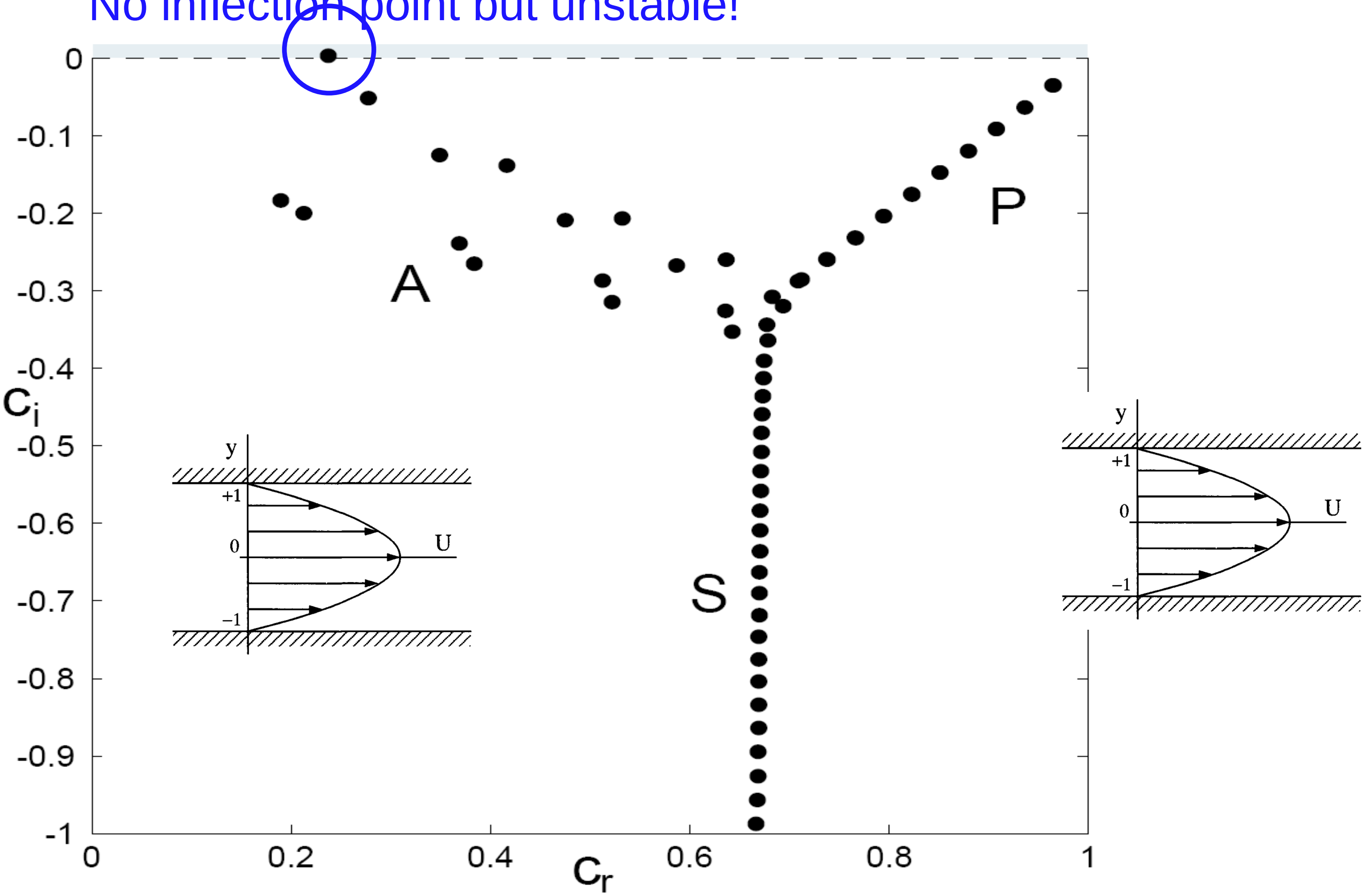

$c=\omega/k$

Eigenfunction and critical layer

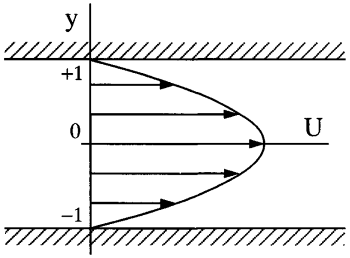

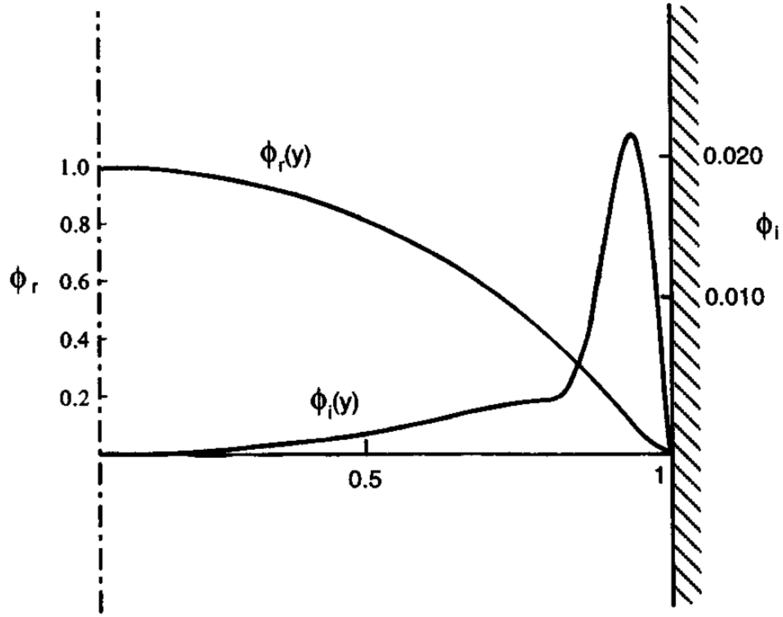

Fig. 8.3. Even eigenfunction at $k = 1$ and Re $= 10^4$ for the eigenvalue $c = 0.23 + 0.0037i$ in plane Poiseuille flow. After Drazin and Reid (1981), original results of Thomas (1953).

Critical layer at y_c where $U(y_c)$~c

$$\boxed{[U(y)-c]}[\phi''-k^2\phi]-U''(y)\,\phi=\frac{1}{i\,k\,Re}\left(\frac{d^2}{dy^2}-k^2\right)^2\phi$$

Eigenfunction and critical layer

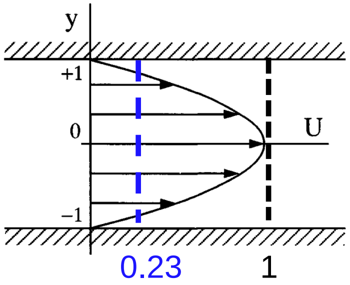

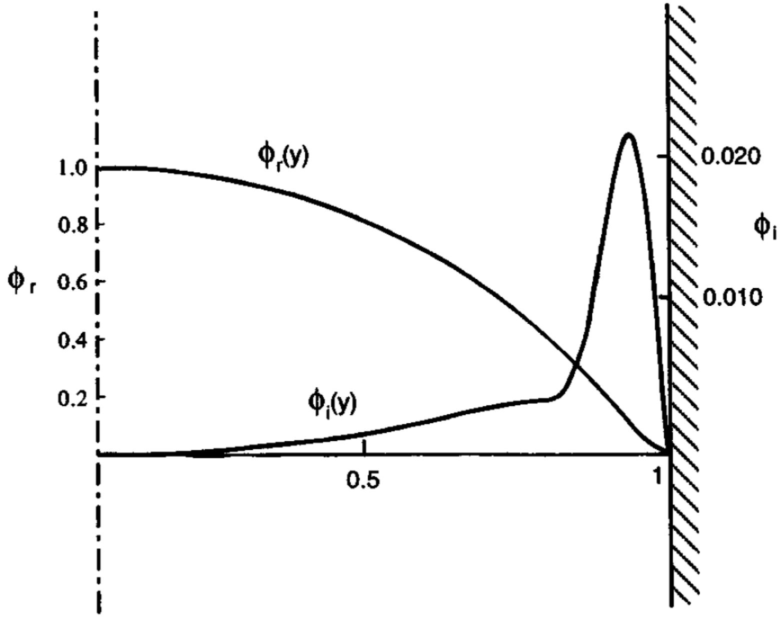

Fig. 8.3. Even eigenfunction at $k = 1$ and $\mathrm{Re} = 10^4$ for the eigenvalue $c = 0.23 + 0.0037i$ in plane Poiseuille flow. After Drazin and Reid (1981), original results of Thomas (1953).

Critical layer at y_c where $U(y_c)\sim c$

$$[U(y) - c][\phi'' - k^2\phi] - U''(y)\,\phi = \frac{1}{i\,k\,Re}\left(\frac{d^2}{dy^2} - k^2\right)^2 \phi$$

Eigenfunction and critical layer

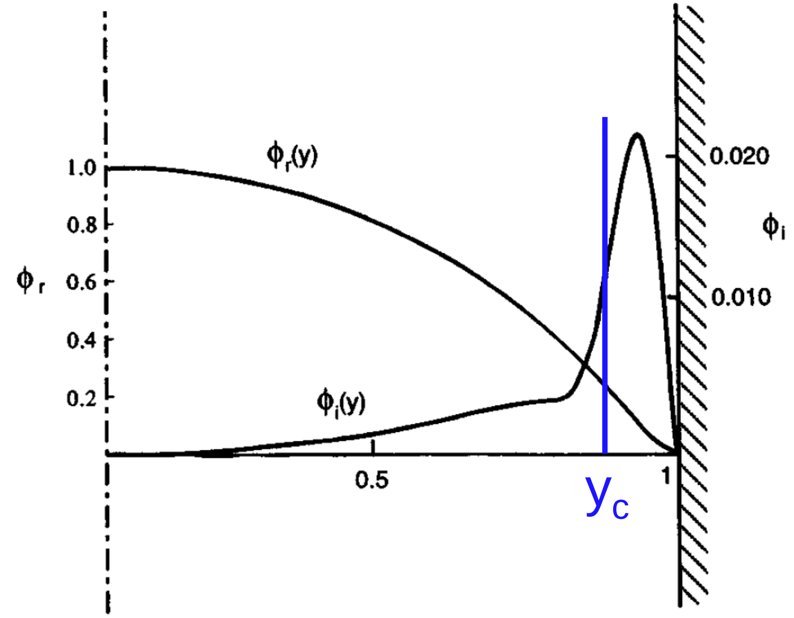

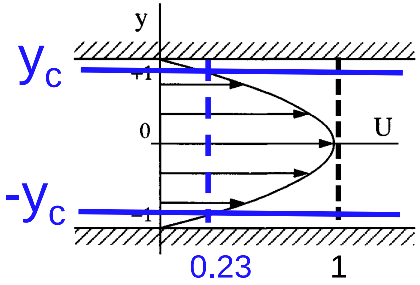

Fig. 8.3. Even eigenfunction at $k = 1$ and Re $= 10^4$ for the eigenvalue $c = \boxed{0.23} + 0.0037i$ in plane Poiseuille flow. After Drazin and Reid (1981), original results of Thomas (1953).

Critical layer at y_c where $U(y_c) \sim c$

$$\boxed{[U(y) - c]}[\phi'' - k^2\phi] - U''(y)\,\phi = \frac{1}{i\,k\,Re}\left(\frac{d^2}{dy^2} - k^2\right)^2 \phi$$

Neutral curve for plane poiseuille flow

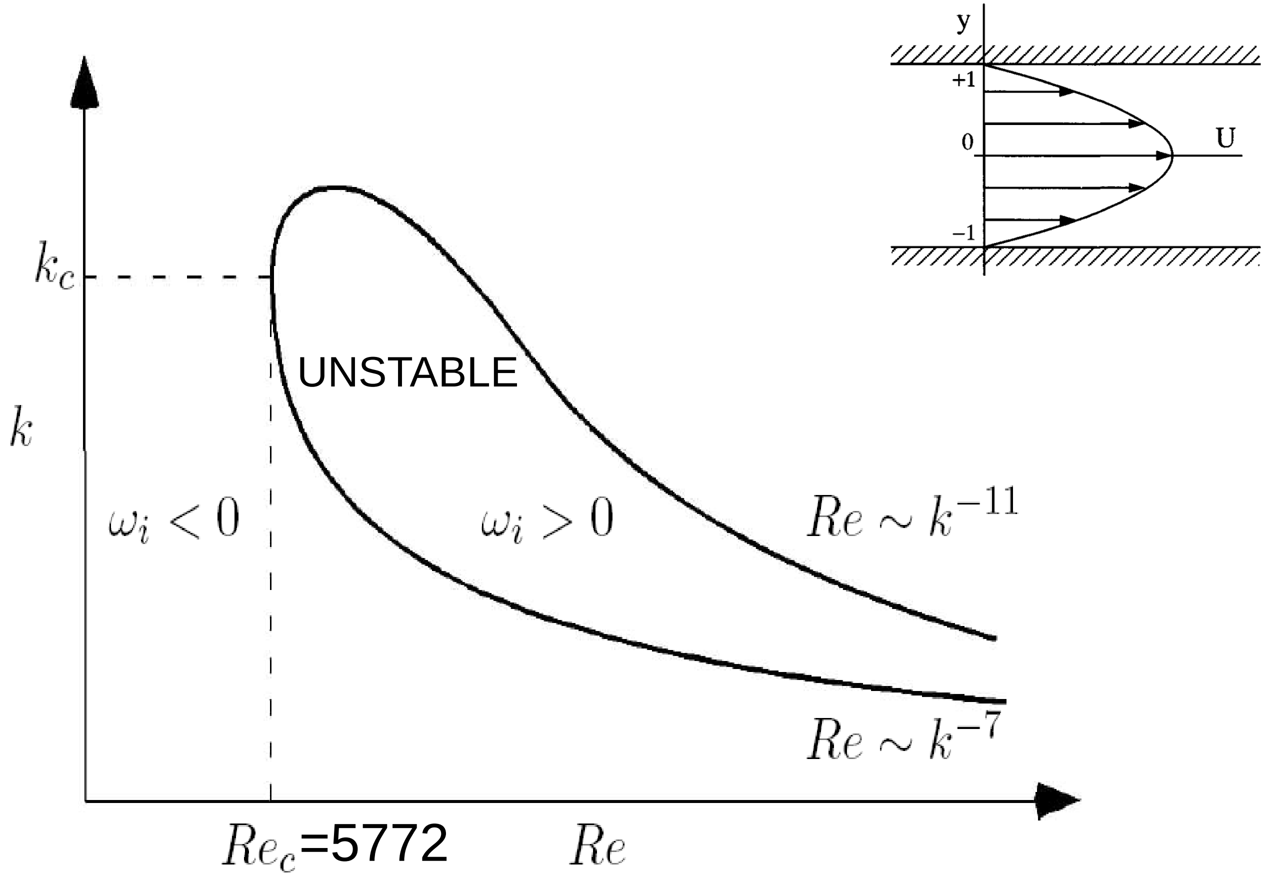

– *Allure de la courbe de stabilité marginale dans le plan* $Re - k$ *pour l'écoulement de Poiseuille plan.*

Poiseuille experiments

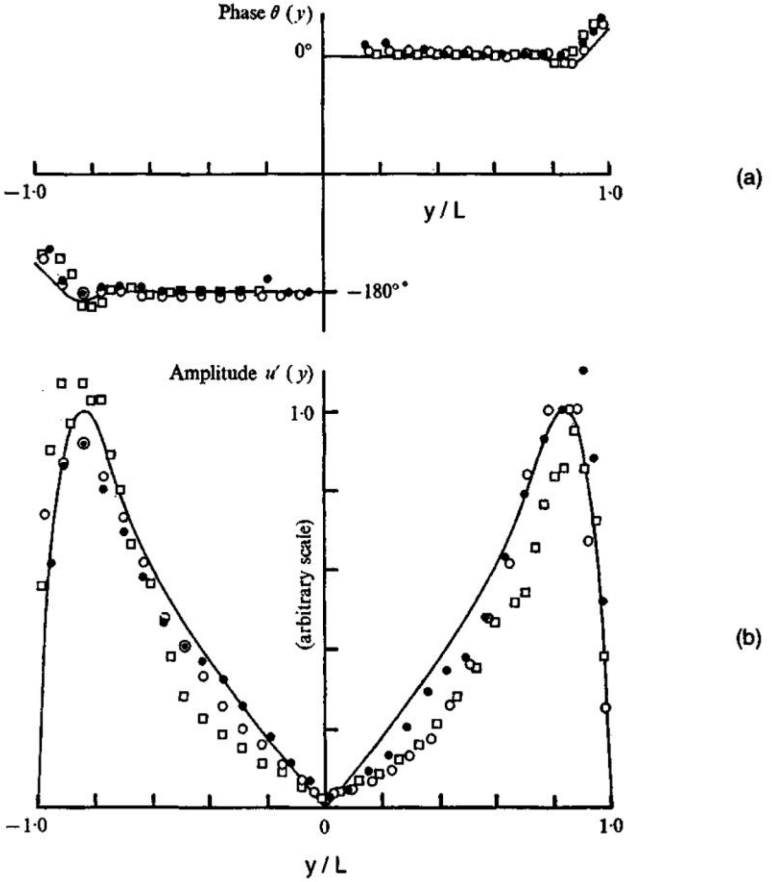

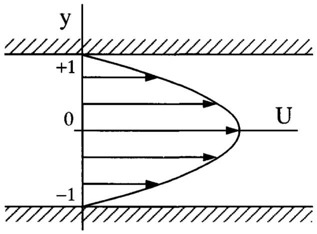

Fig. 2.20. Measured phase (a) and amplitude (b) cross-stream distribution of streamwise perturbation velocities in plane Poiseuille flow. Continuous curves are Itoh's corresponding predictions (1974) for spatially evolving Tollmien–Schlichting waves at $\omega = 0.27$ and $\mathrm{Re} = 4,000$ (see section 8.1). Experimental conditions of Nishioka *et al.* (1975): open circles: $\mathrm{Re} = 3,000$, $\omega = 0.36$; solid circles: $\mathrm{Re} = 4,000$, $\omega = 0.27$; squares: $\mathrm{Re} = 6,000$, $\omega = 0.32$.

Poiseuille experiments

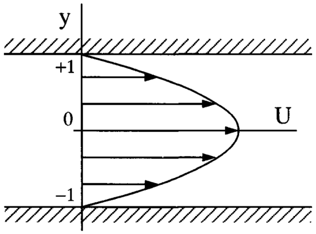

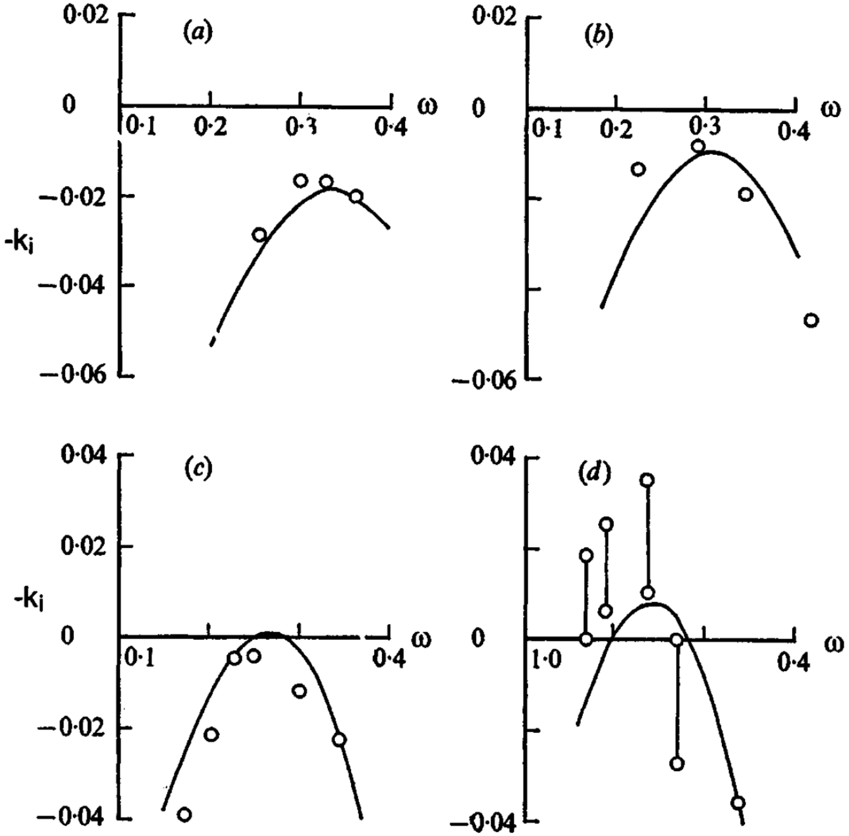

Fig. 8.5. Spatial amplification rates $-k_i$ versus frequency ω (Nishioka *et al.*, 1975). —: Itoh's theoretical prediction (1974); ○: experiments. (a): Re = 3,000. (b): Re = 4,000. (c): Re = 6,000; experiments: Re = 5,700. (d): Re = 8,000; experiments: Re = 7,000.

Boundary layers are destabilized by viscosity
Reynolds Orr equation

Perturbation kinetic energy: $e_c = \frac{1}{2}(u^2 + v^2 + w^2)$

$$\frac{\mathrm{d}}{\mathrm{d}t}\int_{y_1}^{y_2}\langle e_c\rangle \mathrm{d}y = \int_{y_1}^{y_2} \partial_y \overline{U}\,\tau_{xy}\mathrm{d}y - \frac{1}{Re}\int_{y_1}^{y_2}\langle \boldsymbol{\omega}.\boldsymbol{\omega}\rangle \mathrm{d}y$$

Production term Dissipation term

$\boldsymbol{\omega} = \boldsymbol{\nabla} \times \mathbf{u}$ is the perturbation vorticity

$$\tau_{xy} \equiv -\overline{uv} = -\tfrac{1}{2}|\hat{u}(y)||\hat{v}(y)|cos[\varphi_u(y) - \varphi_v(y)]\,\mathrm{e}^{2kc_it}\,,$$

$$\hat{u}(y) \equiv |\hat{u}(y)|\,\mathrm{e}^{i\varphi_u(y)}\,, \qquad \hat{v}(y) \equiv |\hat{v}(y)|\,\mathrm{e}^{i\varphi_v(y)}\,.$$

Boundary layers are destabilized by viscosity
Reynolds Orr equation

Perturbation kinetic energy: $e_c = \frac{1}{2}(u^2 + v^2 + w^2)$

$$\frac{\mathrm{d}}{\mathrm{d}t}\int_{y_1}^{y_2}\langle e_c\rangle \mathrm{d}y = \boxed{\int_{y_1}^{y_2} \partial_y \overline{U}\tau_{xy}\mathrm{d}y} - \boxed{\frac{1}{Re}\int_{y_1}^{y_2}\langle \boldsymbol{\omega}.\boldsymbol{\omega}\rangle \mathrm{d}y}$$

Production term Dissipation term

$\boldsymbol{\omega} = \boldsymbol{\nabla} \times \mathbf{u}$ is the perturbation vorticity

$$\tau_{xy} \equiv -\overline{uv} = -\frac{1}{2}|\hat{u}(y)||\hat{v}(y)|cos[\varphi_u(y) - \varphi_v(y)]\, \mathrm{e}^{2kc_it} \,,$$

$$\hat{u}(y) \equiv |\hat{u}(y)|\, \mathrm{e}^{i\varphi_u(y)} \,, \qquad \hat{v}(y) \equiv |\hat{v}(y)|\, \mathrm{e}^{i\varphi_v(y)} \,.$$

For invisicd flow $\varphi_u(y) - \varphi_v(y) = \pm\pi/2 \rightarrow \tau_{xy} \equiv 0 \rightarrow$ the production term is 0

For viscous flow if $\varphi_u(y) - \varphi_v(y) \neq \pm\pi/2 \rightarrow$ production term can be positive

Tollmien Schlichting waves

Schmid and Henningson 2002

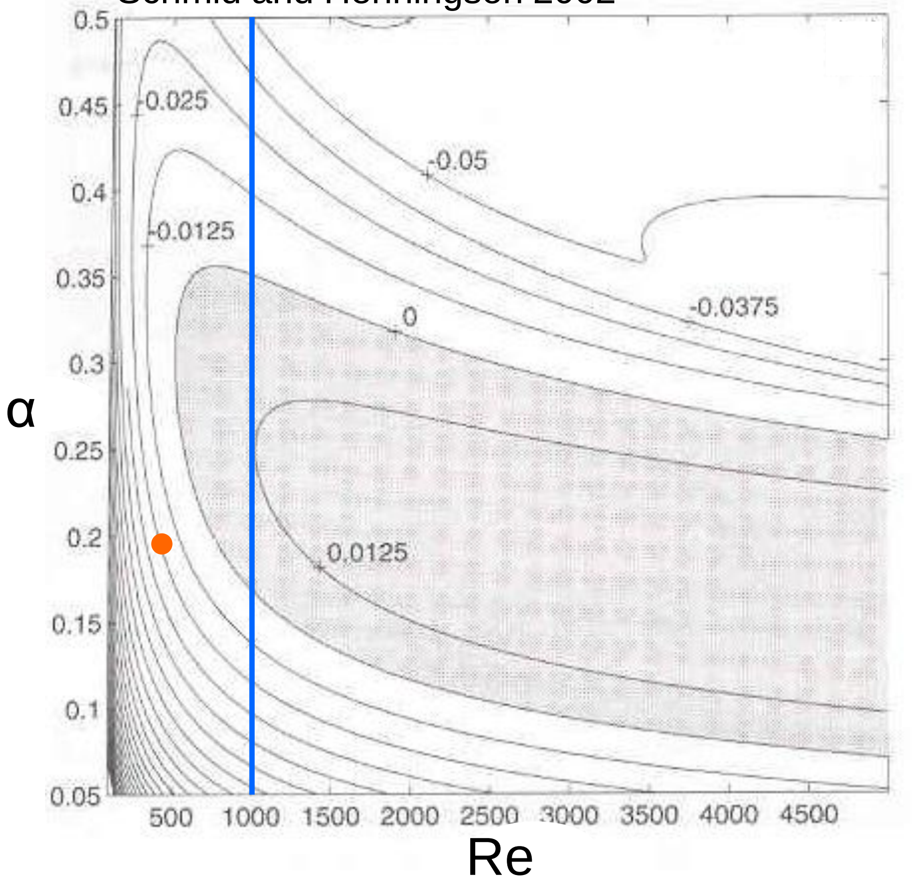

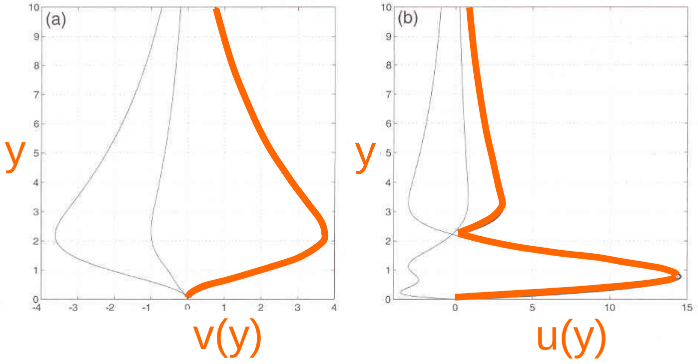

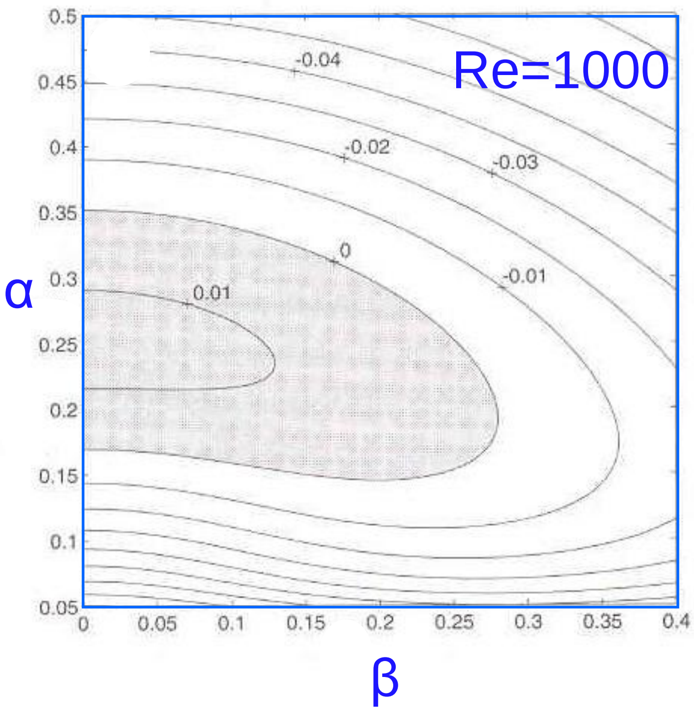

α: axial wavenumber

β: transverse wavenumber

Local parallel flow approximation

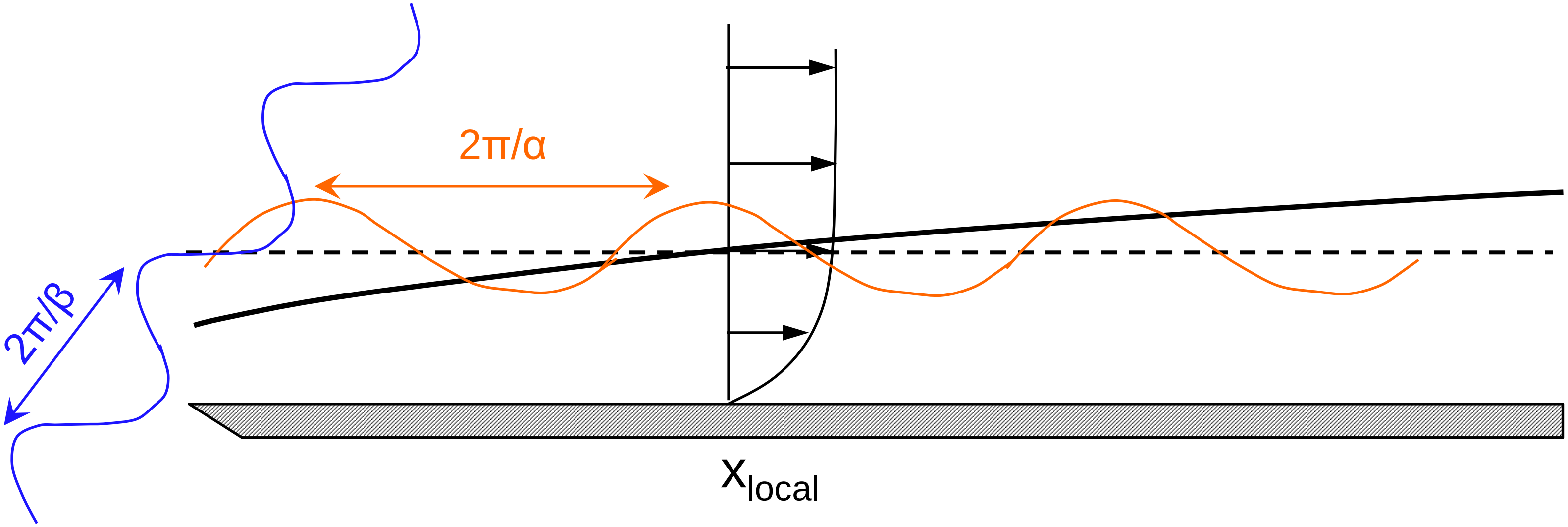

$$(\mathbf{u}, p) = (\mathbf{u}(y), p(y))\, \mathrm{e}^{\sigma t + i(\alpha x + \beta z)}$$

⇨Orr-Sommerfeld-Squire equation

$$\frac{\partial \mathbf{u}}{\partial t} + \mathbf{U}(y)\nabla \mathbf{u} + \mathbf{u}\nabla \mathbf{U}(y) = -\nabla p + \frac{1}{Re}\nabla^2 \mathbf{u}$$
$$\nabla.\mathbf{u} = 0$$

Boundary layer at increasing Reynolds number

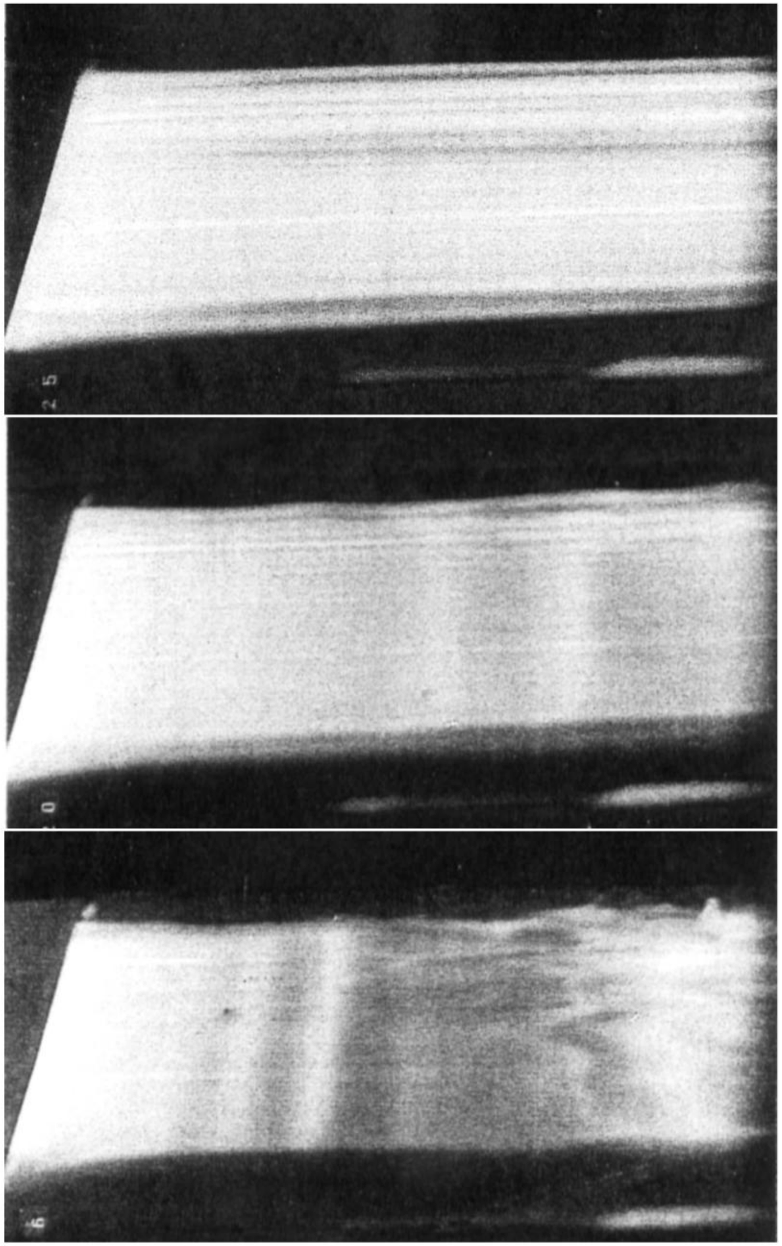

Neutral curve

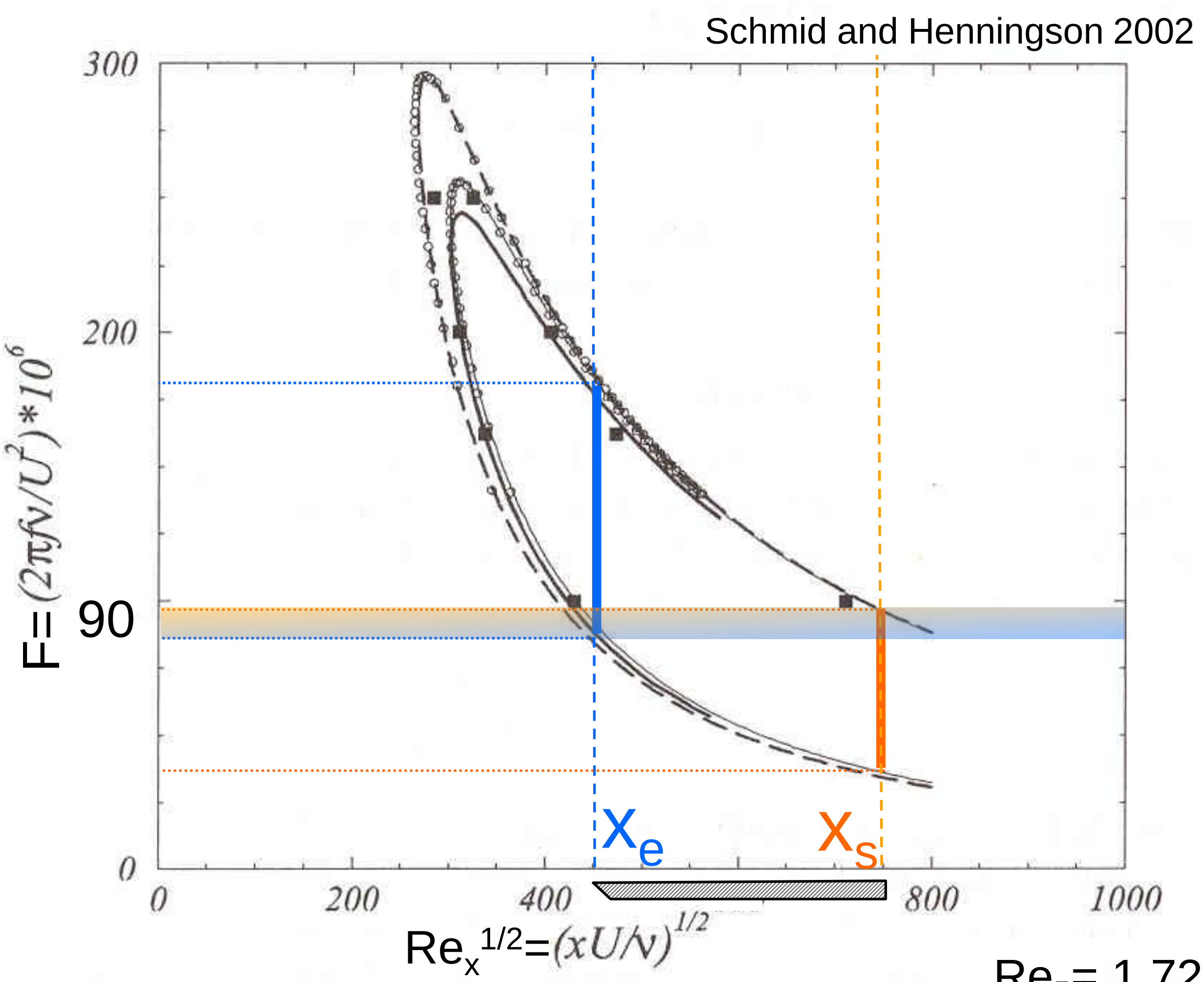

$Re_\delta= 1.72Re_x^{1/2}$

Boundary layer at Re_δ =1500

Growth-rate

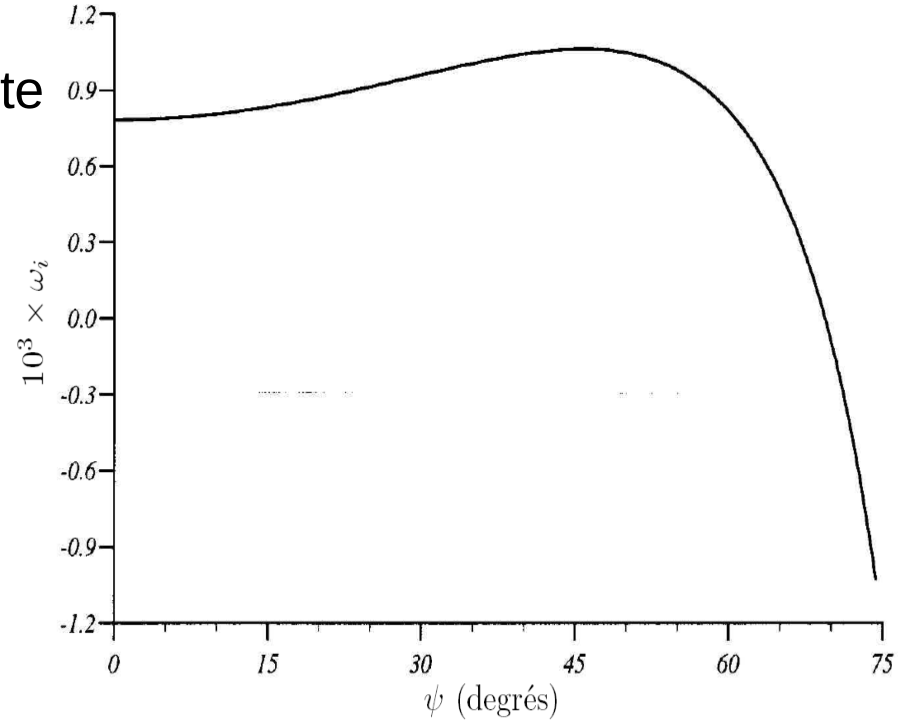

ψ= tan(β/α)

Taux de croissance temporel (s^{-1}) *de l'instabilité d'une couche limite, en fonction de l'angle* ψ *de la perturbation avec la direction de l'écoulement de base.* $R_{\delta 1} = 1500$, $\omega\nu/U_\infty^2 = 0,3 \times 10^{-4}$ *(calcul G. Casalis, ONERA).*

The most unstable perturbation is oblique!

Hagen Poiseuille

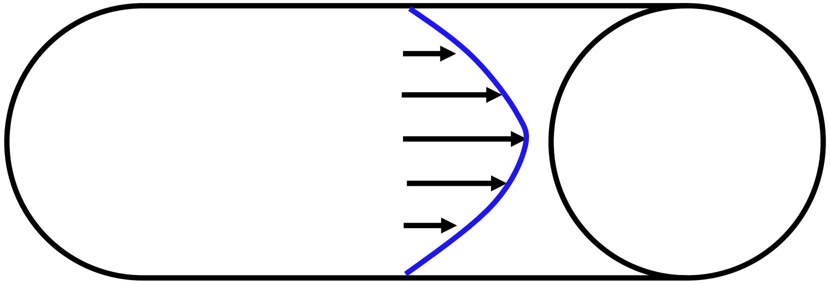

Couette

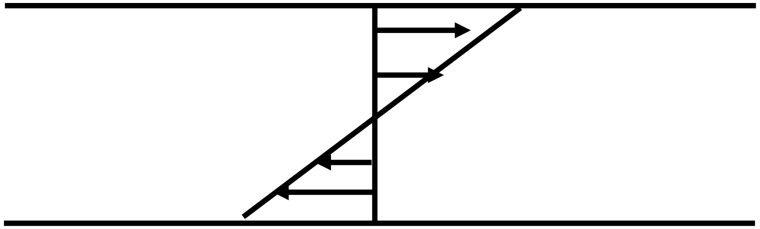

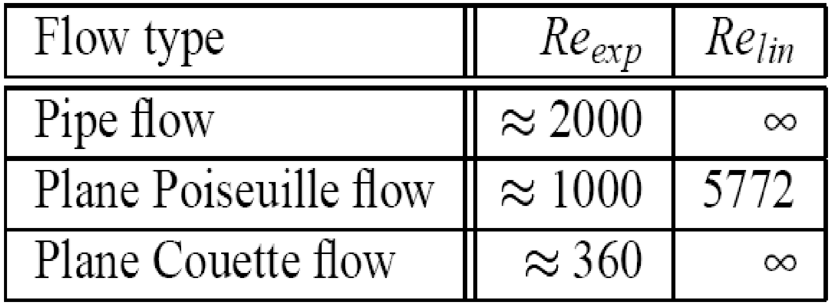

Flow type	Re_{exp}	Re_{lin}
Pipe flow	≈ 2000	∞
Plane Poiseuille flow	≈ 1000	5772
Plane Couette flow	≈ 360	∞

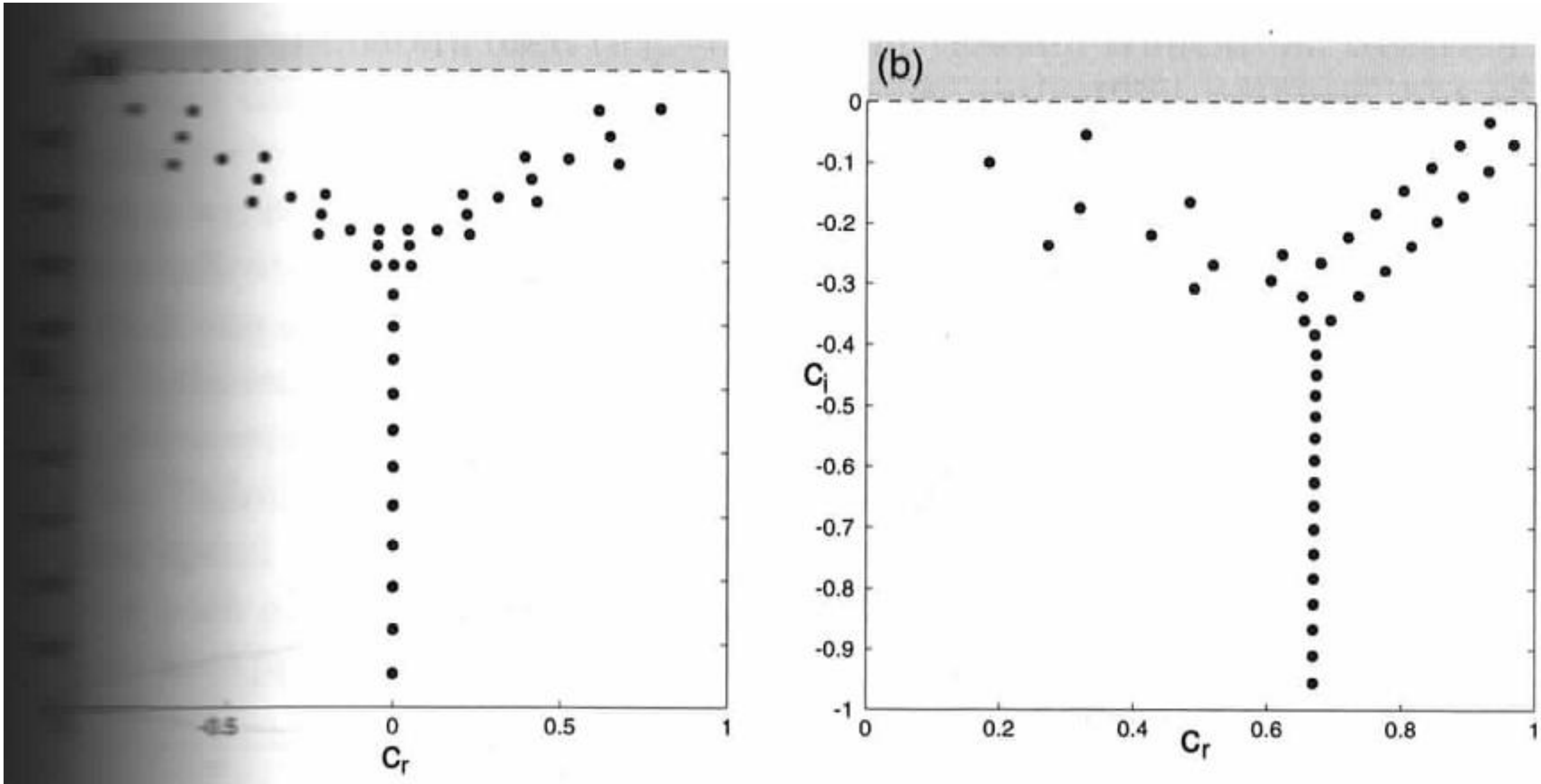

FIGURE 3.3. Spectrum of plane Couette and pipe flow. (a) Plane Couette flow for $\alpha = 1, \beta = 1, \mathrm{Re} = 1000$; (b) Pipe flow for $\alpha = 1, n = 1, \mathrm{Re} = 5000$.

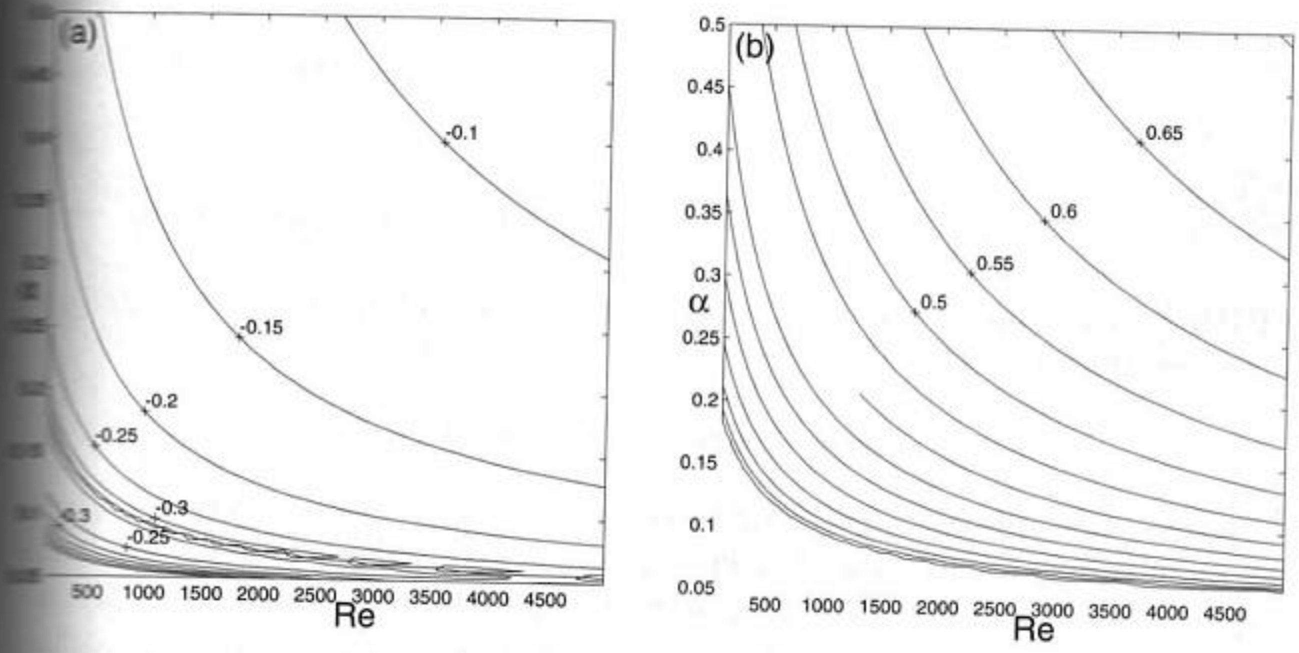

FIGURE 3.11. Contours of constant growth rate (a) and phase speed (b) for plane Couette flow.

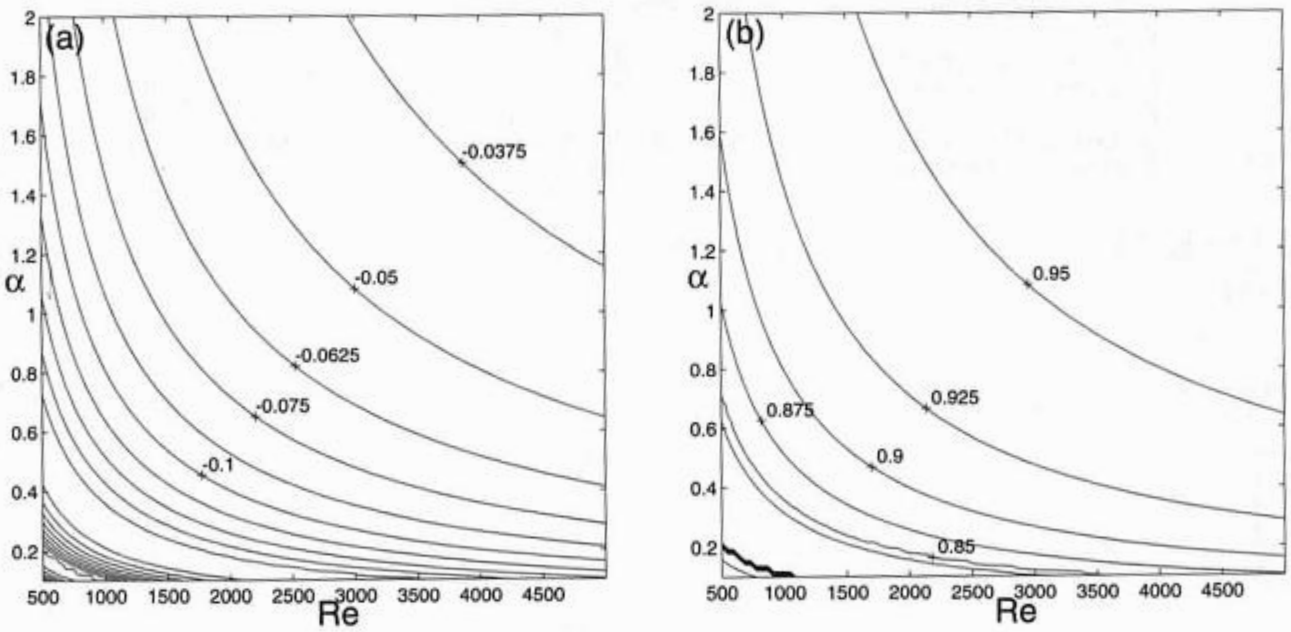

FIGURE 3.12. Contours of constant growth rate (a) and phase speed (b) for pipe Poiseuille flow.

What about nonlinearities?

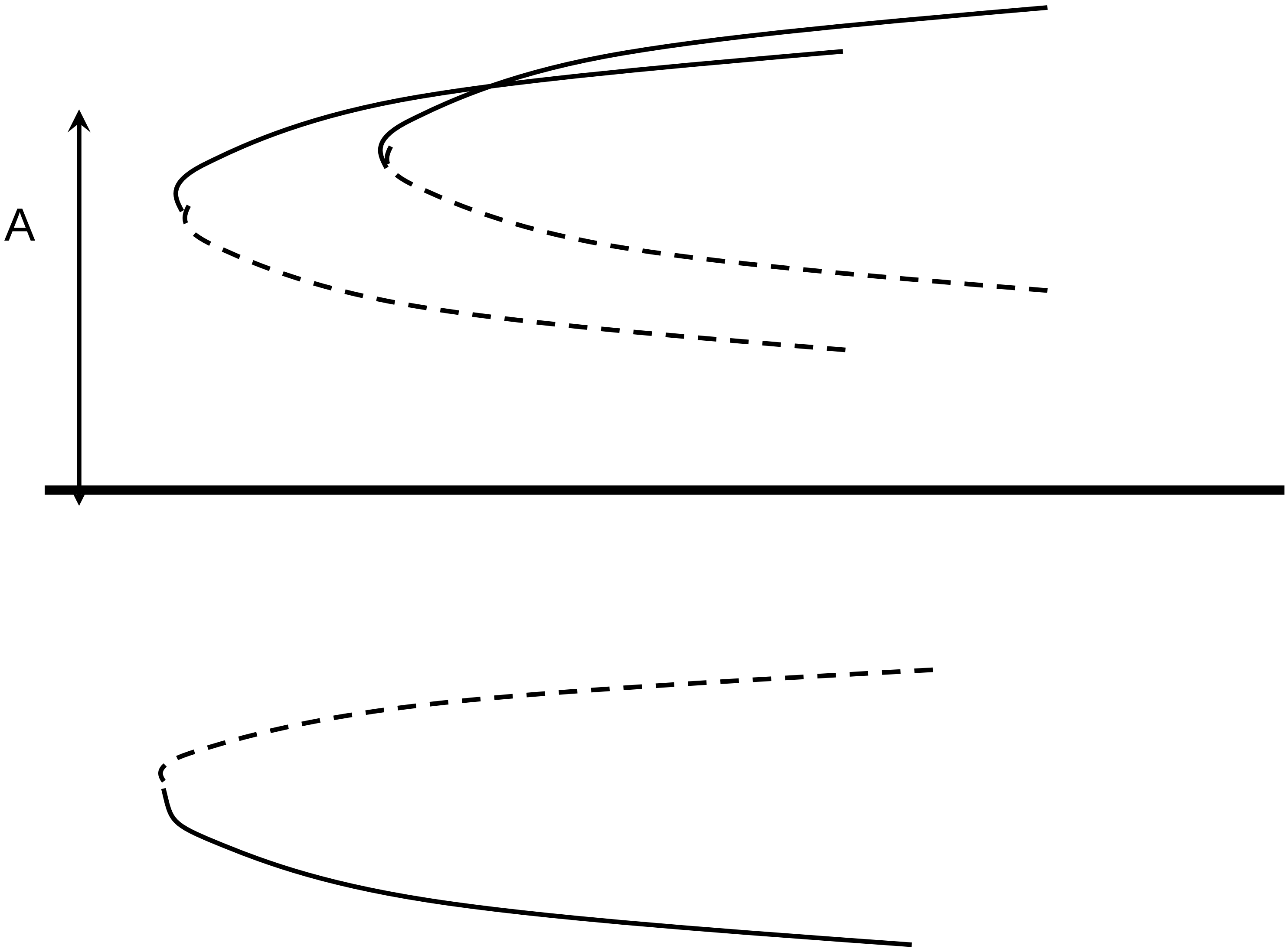

Edge states

Transient growth and bye pass transition

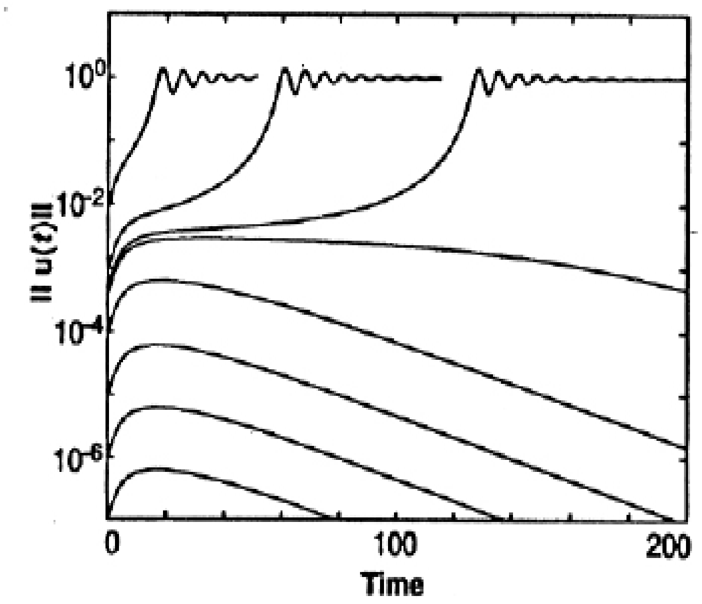

Conditional stability – subcritical bifurcation
Trefethen 1993

$$\mathbf{B} = \begin{bmatrix} -1 & 5 \\ 0 & -2 \end{bmatrix}$$

$$\mathbf{A} = \begin{bmatrix} -1 & 0 \\ 0 & -2 \end{bmatrix}$$

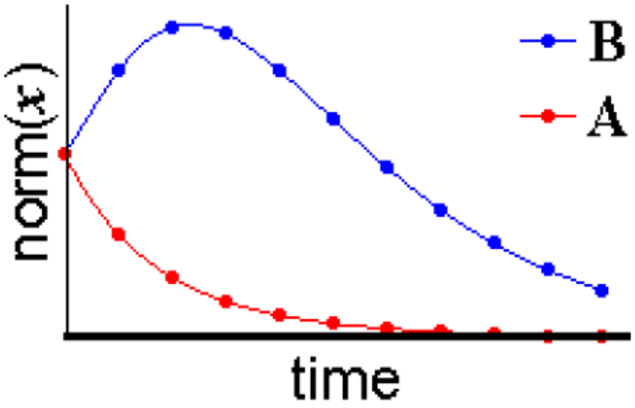

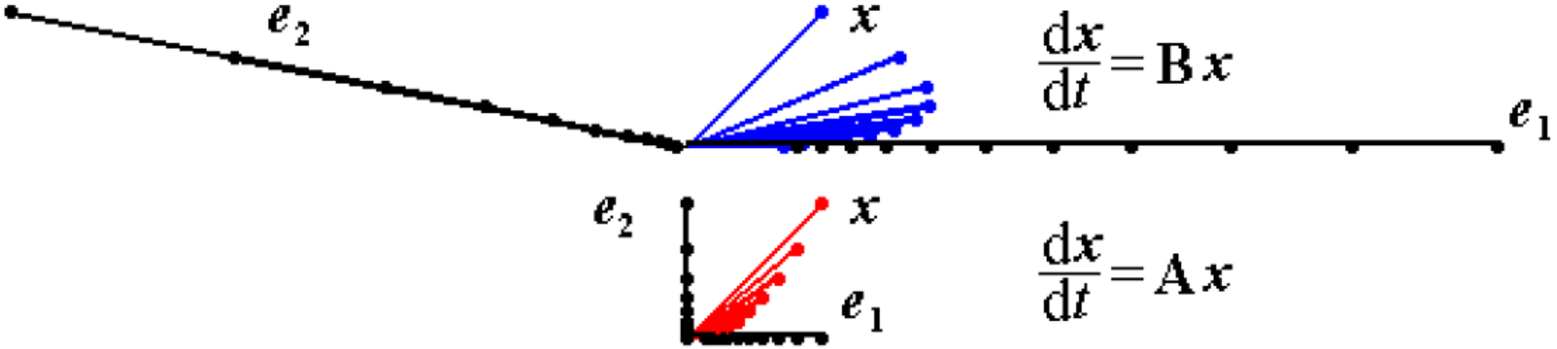

$$\frac{\mathrm{d}\boldsymbol{x}}{\mathrm{d}t} = \mathbf{B}\,\boldsymbol{x}$$

$$\frac{\mathrm{d}\boldsymbol{x}}{\mathrm{d}t} = \mathbf{A}\,\boldsymbol{x}$$

Eigenvalues and eigenfunctions

λ_1

$$\mathbf{B} = \begin{bmatrix} \boxed{-1} & 5 \\ 0 & \boxed{-2} \end{bmatrix}$$

λ_2

$$V_1 = \begin{bmatrix} 1 \\ 0 \end{bmatrix}$$

$$V_2 = \begin{bmatrix} -0.98 \\ 0.19 \end{bmatrix}$$

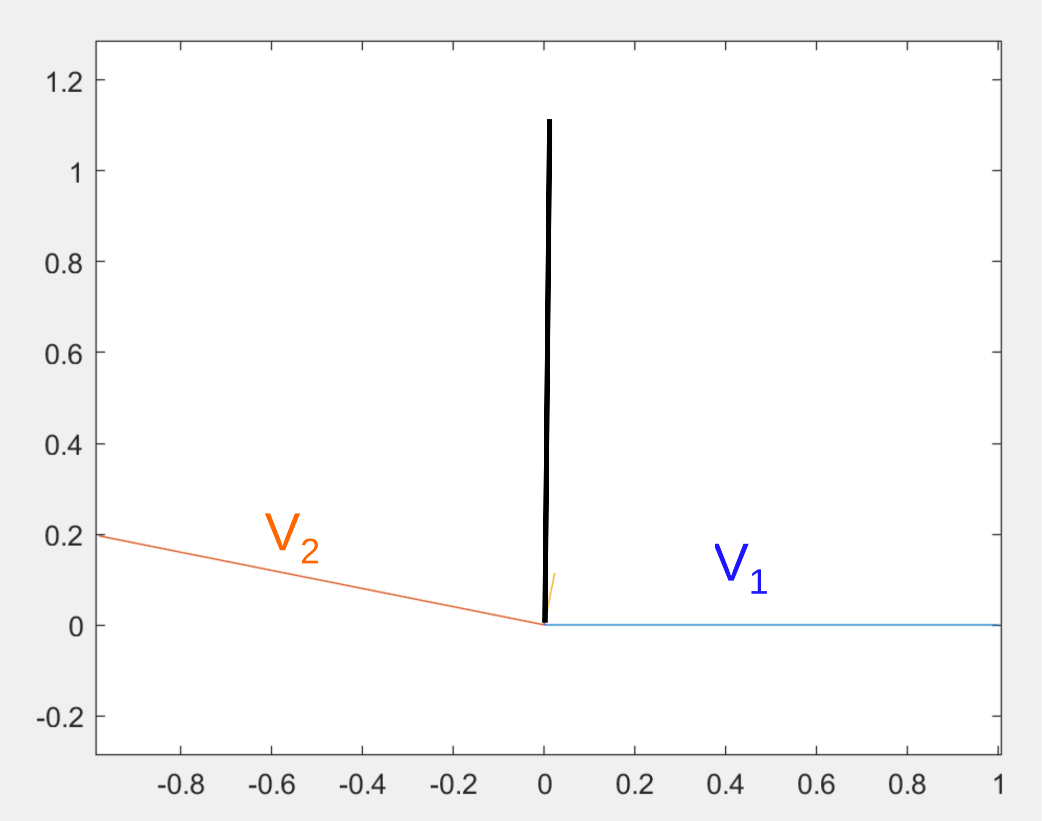

Eigenvalues and eigenfunctions

$$\mathbf{B} = \begin{bmatrix} \overset{\lambda_1}{\boxed{-1}} & 5 \\ 0 & \underset{\lambda_2}{\boxed{-2}} \end{bmatrix}$$

$$V_1 = \begin{bmatrix} 1 \\ 0 \end{bmatrix}$$

$$V_2 = \begin{bmatrix} -0.98 \\ 0.19 \end{bmatrix}$$

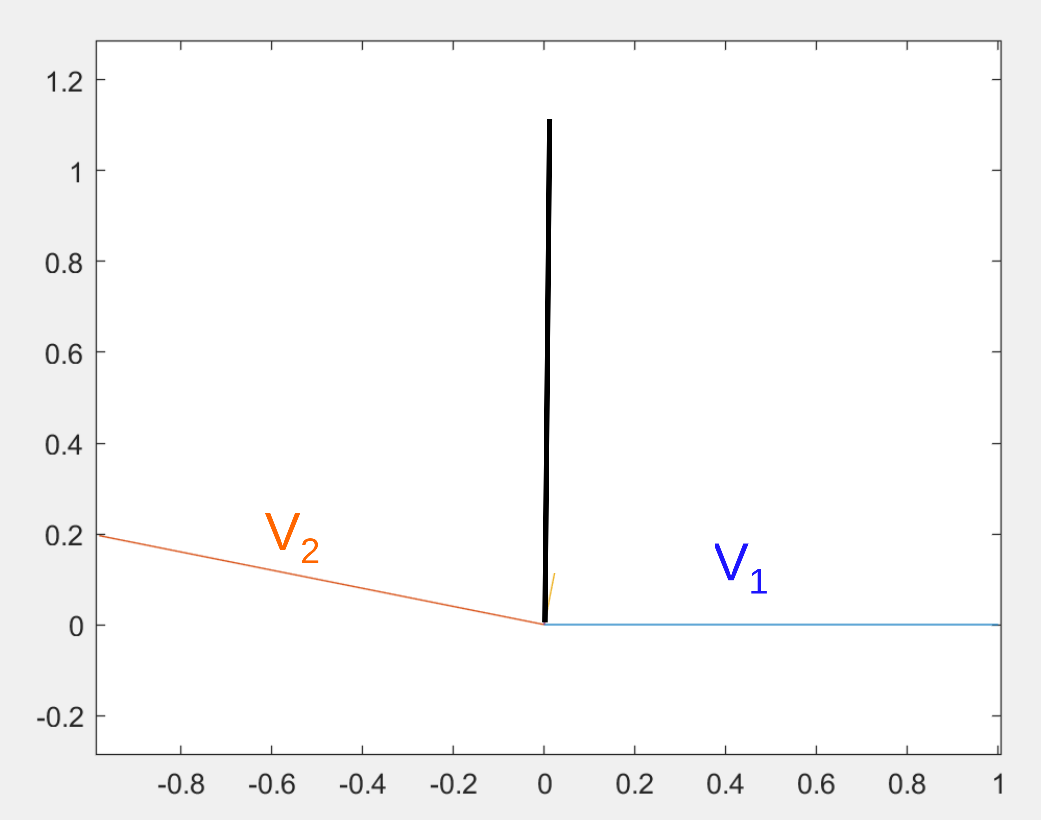

$< V_1, V_2 > = -0.98$

$< V_1, V_1 > = 1$

$< V_2, V_2 > = 1$

Non-orthogonal eigenbasis ⇔ non-normal system

Bi-orthogonal basis and adjoint vectors

$$\mathbf{B} = \begin{bmatrix} \overset{\lambda_1}{-1} & 5 \\ 0 & \underset{\lambda_2}{-2} \end{bmatrix}$$

$$V_1=\begin{bmatrix}1\\0\end{bmatrix}$$

$$V_2=\begin{bmatrix}-0.98\\0.19\end{bmatrix}$$

$$V_2^+=\begin{bmatrix}0\\1\end{bmatrix}$$

$$V_1^+=\begin{bmatrix}0.19\\0.98\end{bmatrix}$$

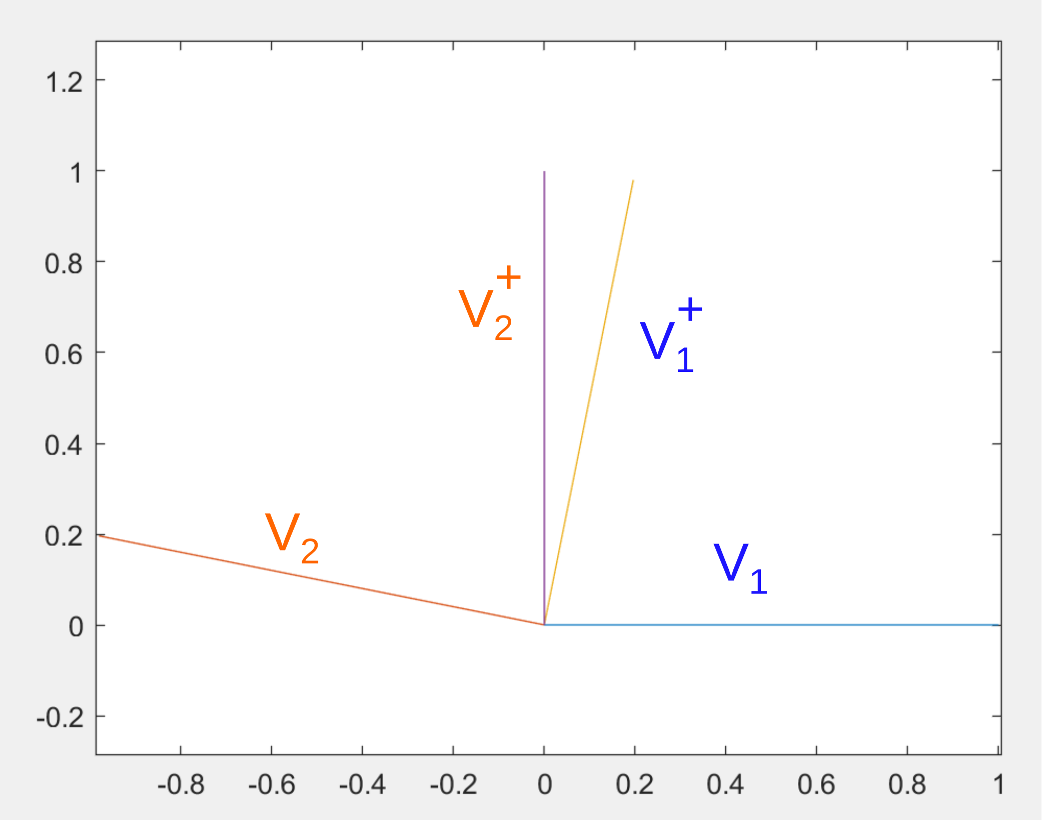

$< V_1,V_2^+> = 0$

$< V_1,V_1^+> = 0.19$

$< V_2,V_2^+> = 0.19$

$< V_2,V_1^+> = 0$

$< V_1,V_1> = 1$

$< V_1^+,V_1^+> = 1$

$< V_2,V_2> = 1$

$< V_2^+,V_2^+> = 1$

$< V_1,V_2> = -0.98$

Projection by scalar product with adjoint vectors

$X_0 = a_1 V_1 + a_2 V_2$

$<X_0, V_1^+> = a_1 <V_1, V_1^+> + a_2 <V_2, V_1^+>$

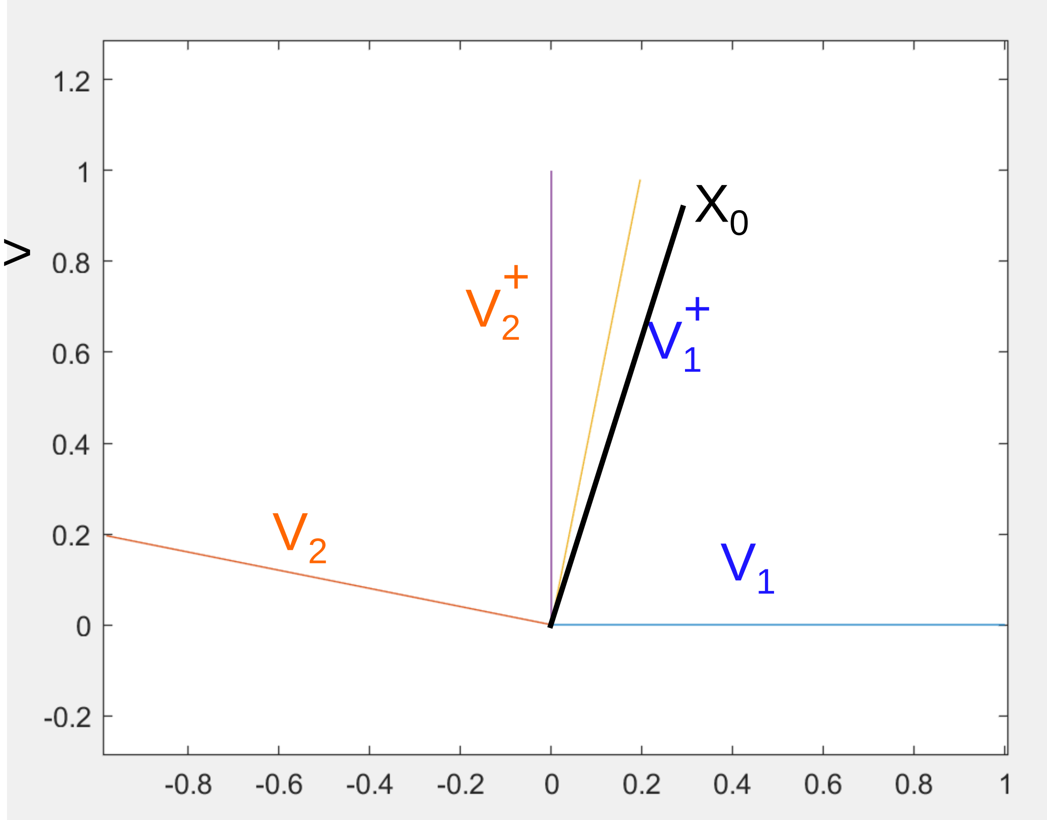

$< V_1, V_2^+> = 0$

$< V_1, V_1^+> = 0.19$

$< V_2, V_2^+> = 0.19$

$< V_2, V_1^+> = 0$

$< V_1, V_1> = 1$

$< V_1^+, V_1^+> = 1$

$< V_2, V_2> = 1$

$< V_2^+, V_2^+> = 1$

Projection by scalar product with adjoint vectors

$X_0=a_1V_1+a_2V_2$

$<X_0,V_1^+>=a_1<V_1,V_1^+>+a_2<\cancel{V_2,V_1^+}>$

$a_1=<X_0,V_1^+> / <V_1,V_1^+>$

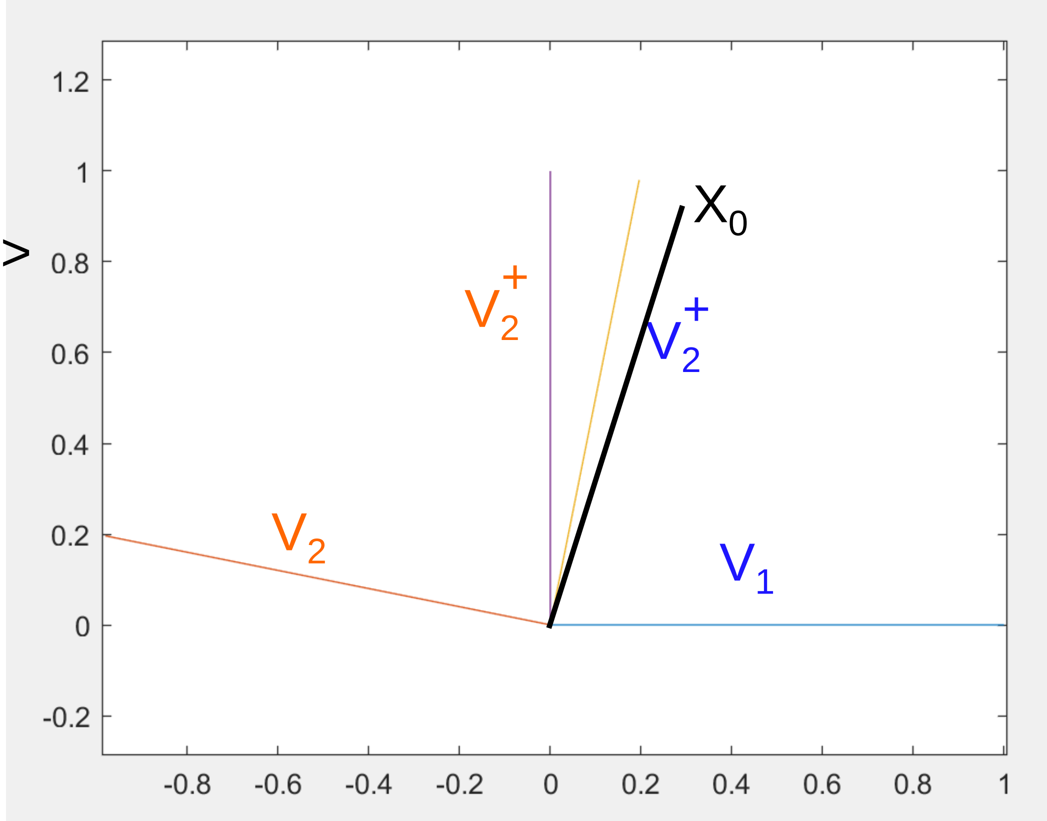

$< V_1,V_2^+> = 0$

$< V_1,V_1^+> = 0.19$

$< V_2,V_2^+> = 0.19$

$< V_2,V_1^+> = 0$

$< V_1,V_1> = 1$

$< V_1^+,V_1^+> = 1$

$< V_2,V_2> = 1$

$< V_2^+,V_2^+> = 1$

Projection by scalar product with adjoint vectors

$X_0=a_1V_1+a_2V_2$

$<X_0,V_1^+>=a_1<V_1,V_1^+>+a_2<\cancel{V_2},V_1^+>$

$a_1=<X_0,V_1^+> / <V_1,V_1^+>$

$a_2=<X_0,V_2^+> / <V_2,V_2^+>$

$X(t)=a_1e^{\lambda 1t}\,V_1+a_2e^{\lambda 2t}\,V_2$

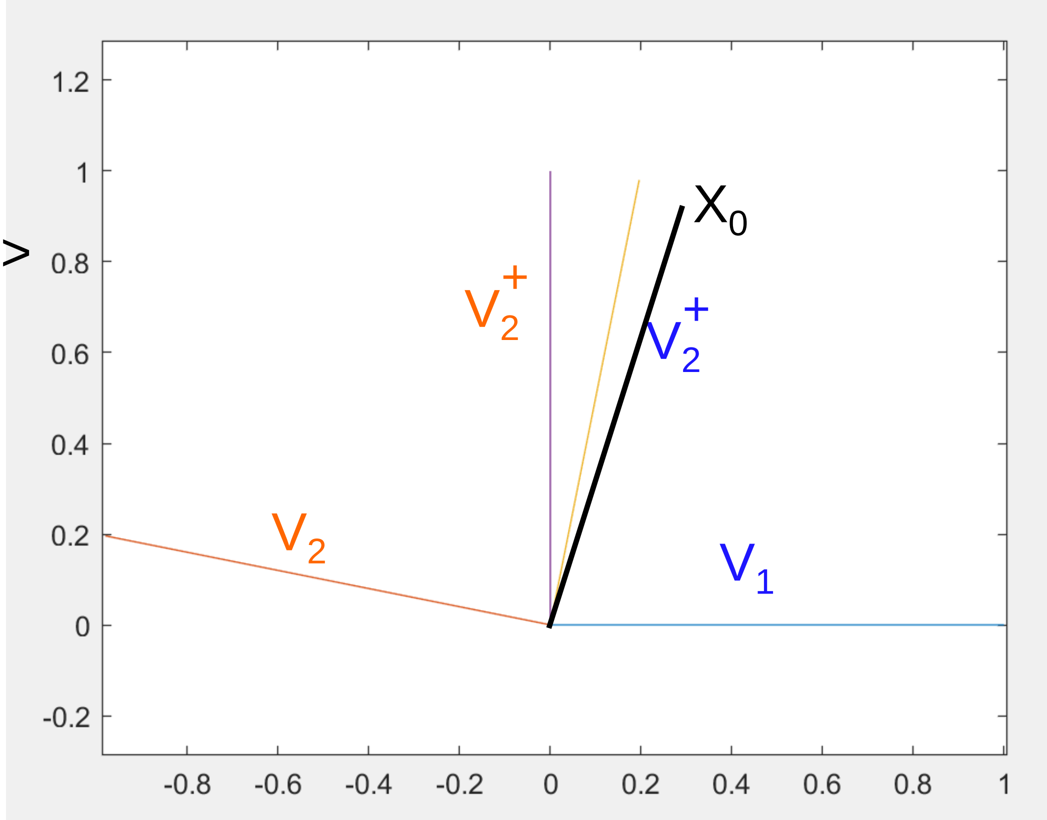

$< V_1,V_2^+> = 0$

$< V_1,V_1^+> = 0.19$

$< V_2,V_2^+> = 0.19$

$< V_2,V_1^+> = 0$

$< V_1,V_1> = 1$

$< V_1^+,V_1^+> = 1$

$< V_2,V_2> = 1$

$< V_2^+,V_2^+> = 1$

Projection by scalar product with adjoint vectors

$$X_0=a_1V_1+a_2V_2$$

$$<X_0,V_1^+>=a_1<V_1,V_1^+>+a_2<\cancel{V_2,V_1^+}>$$

$$a_1=<X_0,V_1^+> / <V_1,V_1^+>$$

$$a_2=<X_0,V_2^+> / <V_2,V_2^+>$$

$$X(t)=a_1e^{\lambda 1t}\,V_1+a_2e^{\lambda 2t}\,V_2$$

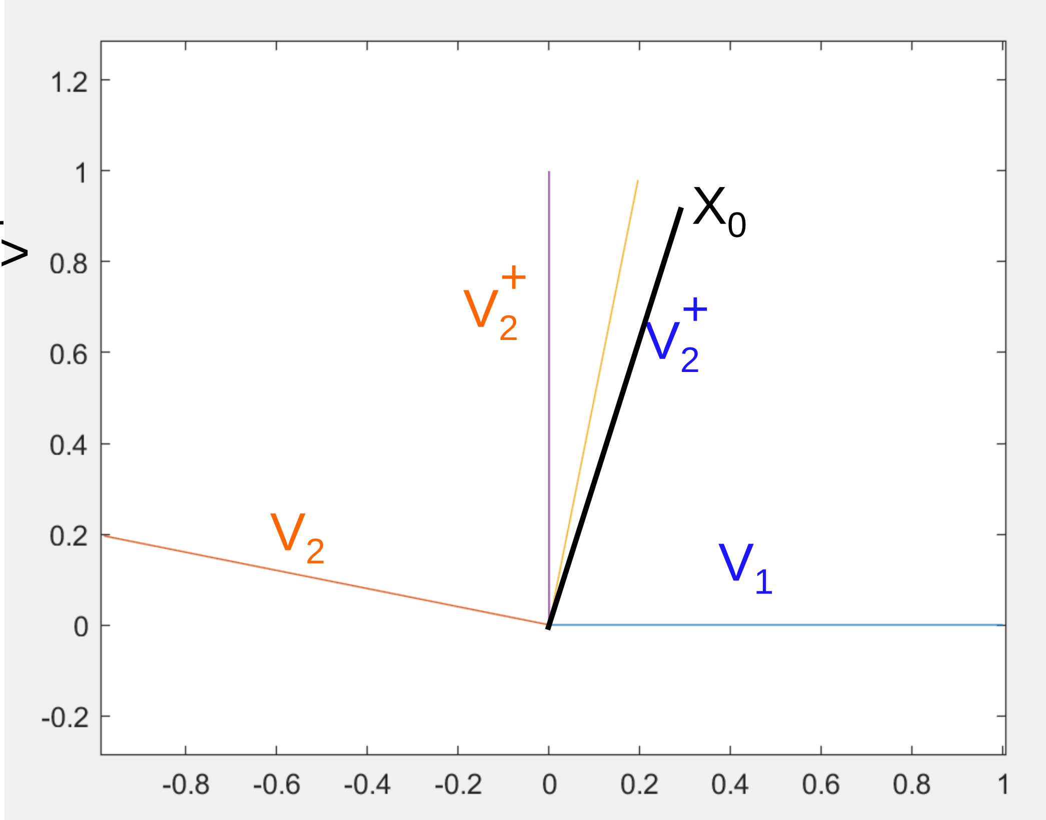

$$||X(t)||^2=a_1^2e^{2\lambda 1t}\,||V_1||^2+a_2^2e^{2\lambda 2t}\,||V_2||^2+a_1a_2 < V_1,V_2>e^{(\lambda 1+\lambda 2)t}$$

Non monotonous energy evolution

$$||X(t)||^2=a_1{}^2e^{2\lambda 1t}\,||V_1||^2+a_2{}^2e^{2\lambda 2t}\,||V_2||^2+a_1a_2 < V_1,V_2>e^{(\lambda 1+\lambda 2)t}$$

$$||X(t)||^2=a_1{}^2e^{2\lambda 1t}+a_2{}^2e^{2\lambda 2t}-0.98\,a_1a_2\,e^{(\lambda 1+\lambda 2)t}$$

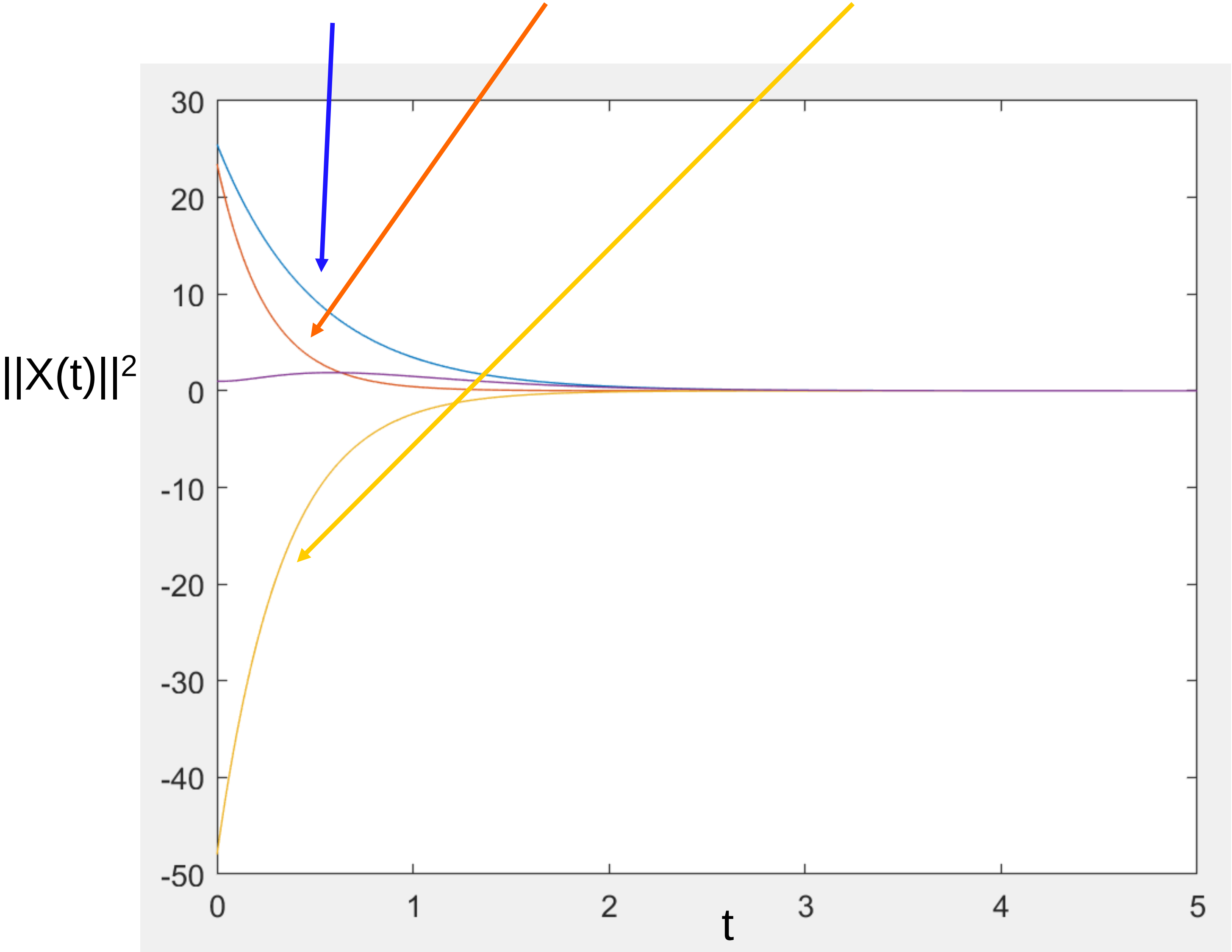

Non-normal growth

$$||X(t)||^2=a_1^2e^{2\lambda1t}\,||V_1||^2+a_2^2e^{2\lambda2t}\,||V_2||^2+a_1a_2 < V_1,V_2>e^{(\lambda1+\lambda2)t}$$

$$||X(t)||^2=a_1^2e^{2\lambda1t}+a_2^2e^{2\lambda2t}-0.98\,a_1a_2\,e^{(\lambda1+\lambda2)t}$$

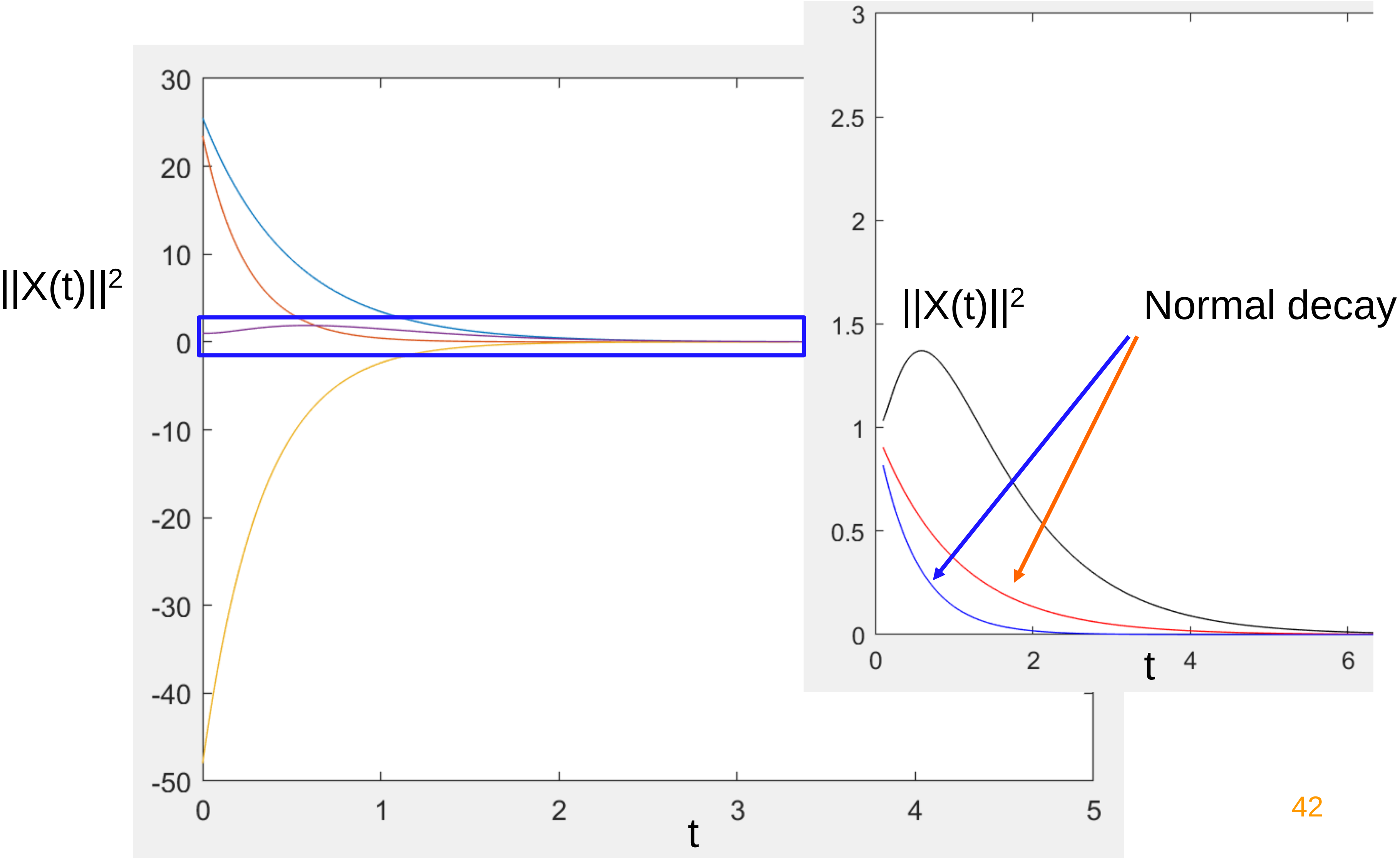

Definition of optimal gain of a linear system

Linear system

$$\frac{dq}{dt} = \mathbf{L}q$$

Initial condition

$$q(t=0) = q_0$$

Optimal gain

$$G(t) \quad = \max_{q_0} \frac{||q||}{||q_0||}$$

?

norm

Definition of optimal gain of a linear system

$$\frac{dq}{dt} = \mathbf{L}q$$

$$q(t = 0) = q_0$$

Matrix exponential

$$q(t) = \exp(\mathbf{L}t)q_0$$

Definition of optimal gain of a linear system

Optimal gain

$$G(t) = \max_{q_0} \frac{||q||}{||q_0||}$$

$$= \max_{q_0} \frac{||\exp(t\mathcal{L})q_0||}{||q_0||}$$

$$= ||\exp(t\mathcal{L})||$$

$$\|x\|_1 = \sum_{i=1}^{m} |x_i|,$$

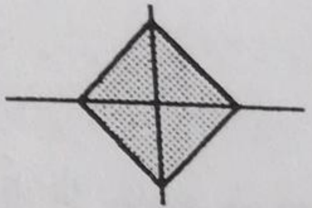

$$\|x\|_2 = \left(\sum_{i=1}^{m} |x_i|^2 \right)^{1/2} = \sqrt{x^* x},$$

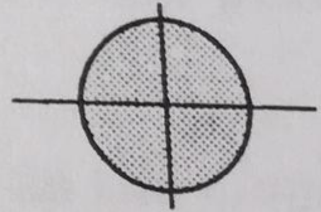

$$\|x\|_\infty = \max_{1 \le i \le m} |x_i|,$$

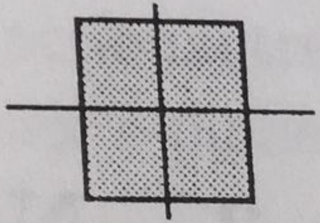

$$\|x\|_p = \left(\sum_{i=1}^{m} |x_i|^p \right)^{1/p} \qquad (1 \le p < \infty).$$

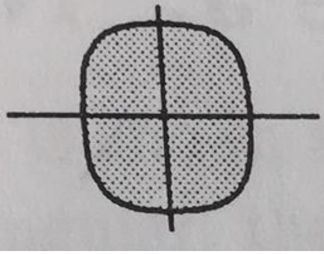

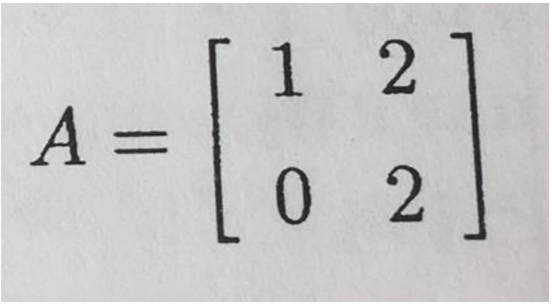

$$A = \begin{bmatrix} 1 & 2 \\ 0 & 2 \end{bmatrix}$$

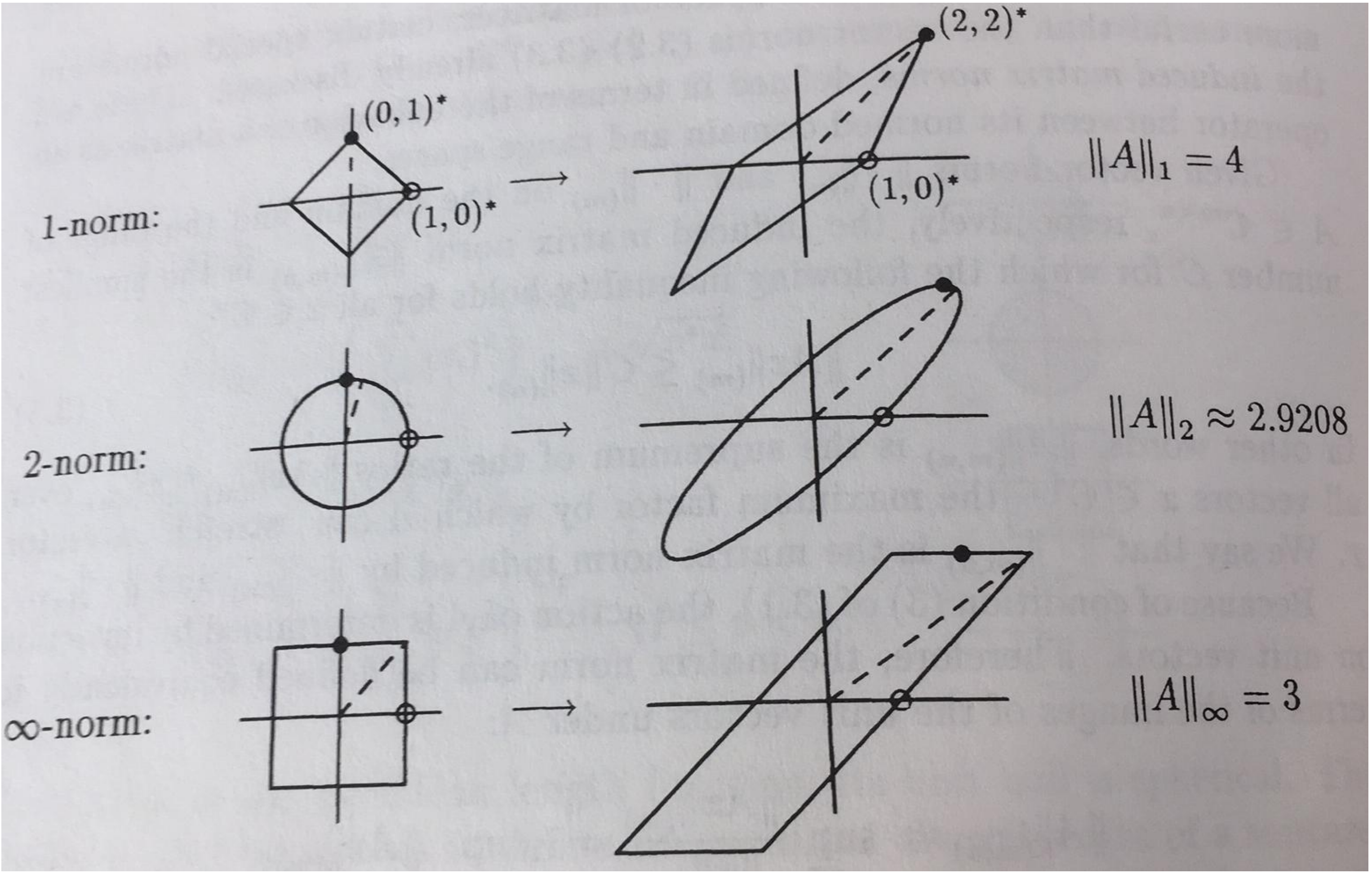

How to compute a matrix 2-norm?

Optimal gain $G(t) = ||\exp(t\mathcal{L})||$

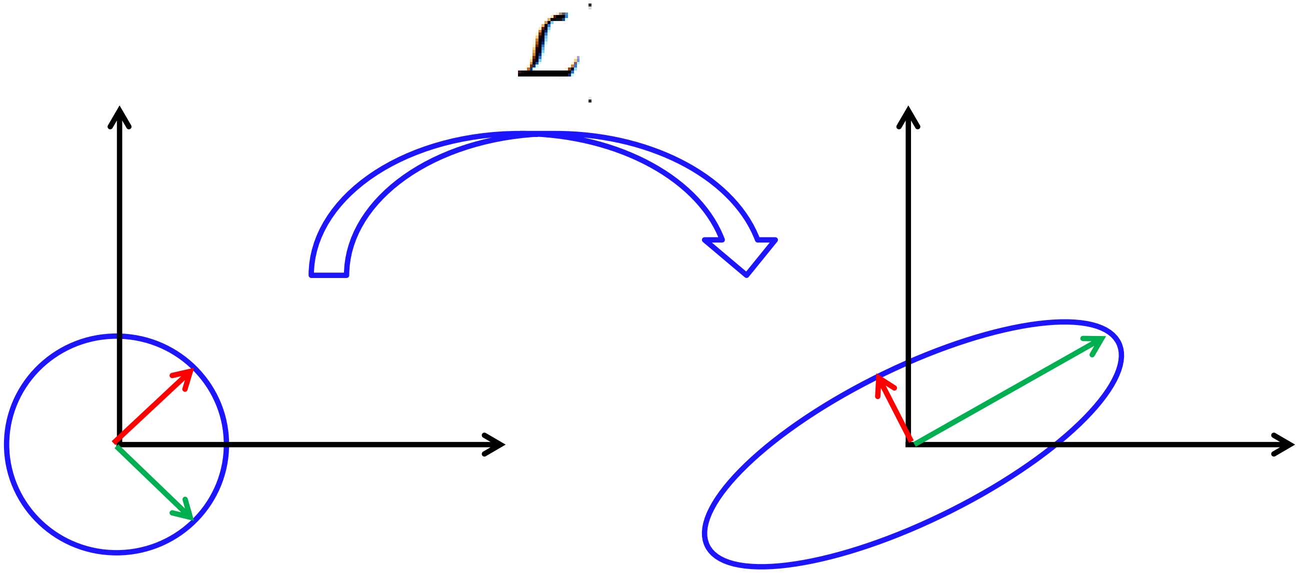

unitary sphere

rotated ellipsoid

Optimal gain is associated to a norm

Kinetic energy written in v,η form

$i\alpha u=Dv-i\beta w$ and $\eta=i\beta u-i\alpha w$

$$E(t) \;=\; \frac{1}{2k^2}\int_{\Omega}\left[|\mathcal{D}v|^2+k^2|v|^2+|\eta|^2\right]\,d\Omega$$

Optimal gain is associated to a norm

Kinetic energy written in v,η form

iαu=Dv-iβw and η=iβu-iαw

$$E(t) = \frac{1}{2k^2}\int_\Omega \left[|\mathcal{D}v|^2 + k^2|v|^2 + |\eta|^2\right] d\Omega$$

$$= \|q\|^2 = \frac{1}{2k^2}\int_\Omega \begin{pmatrix} v \\ \eta \end{pmatrix}^H \begin{pmatrix} -\mathcal{D}^2 + k^2 & 0 \\ 0 & 1 \end{pmatrix} \begin{pmatrix} v \\ \eta \end{pmatrix} d\Omega$$

$$= \frac{1}{2k^2}\int_\Omega q^H M q \, d\Omega$$

energy matrix

Definition of optimal gain of a linear system

Cholevski dec. $M = F^H F$

$$||q||^2 = \frac{1}{2k^2} \int_\Omega q^H F^H F q \, d\Omega = \frac{1}{2k^2} \int_\Omega (Fq)^H F q \, d\Omega$$

Optimal gain

$$\begin{aligned} G(t) &= \max_{q_0} \frac{||q||_E}{||q_0||_E} = \max_{q_0} \frac{||Fq||_2}{||Fq_0||_2} = \max_{q_0} \frac{||F \exp(tL) q_0||_2}{||Fq_0||_2} \\ &= \max_{q_0} \frac{||F \exp(tL) F^{-1} \boxed{F q_0}||_2}{||\boxed{F q_0}||_2} = ||F \exp(tL) F^{-1}||_2 \end{aligned}$$

$=q'_0$

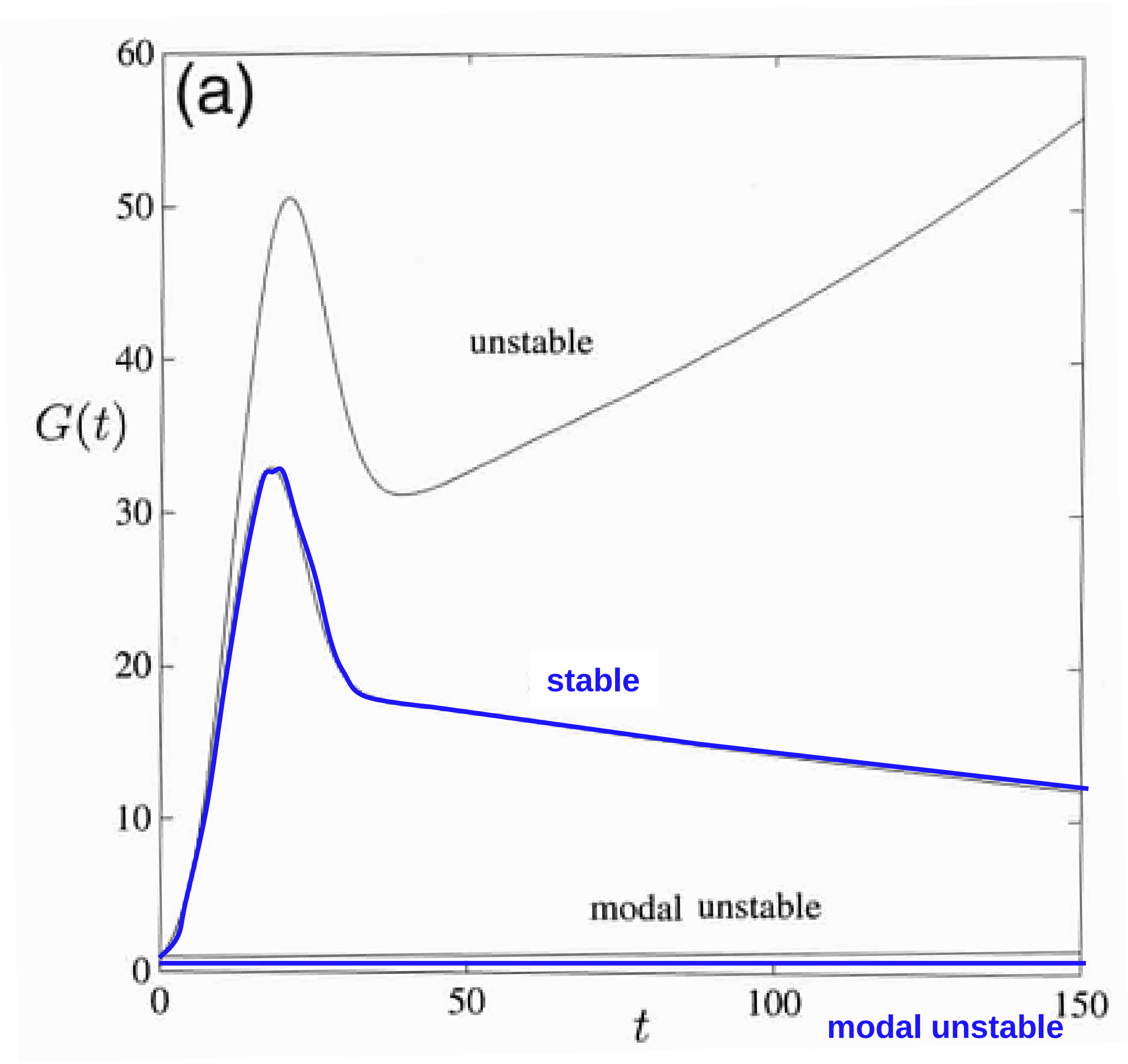
(a)
60
50
40
30
20
10
0
G(t)
unstable
stable
modal unstable
modal unstable
0
50
100
150
t

Plane Poiseuille flow

normal

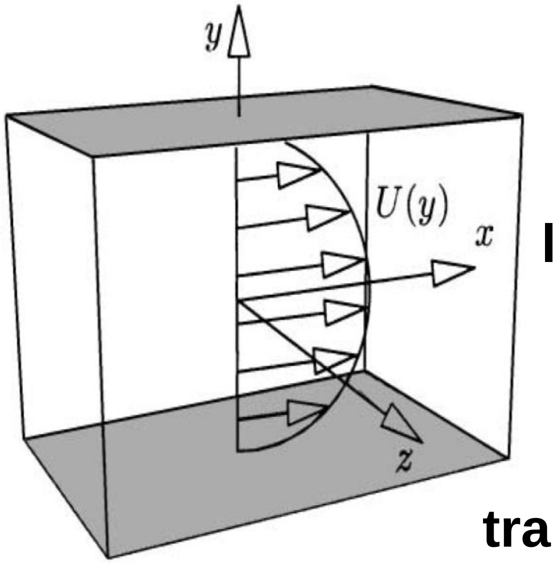

longitudinal, $e^{i\alpha x}$

transverse, $e^{i\beta z}$

Linearly stable until Re=5772, but the transition is observed experimentally close to Re=1000-2000!

Plane Poiseuille flow - stability

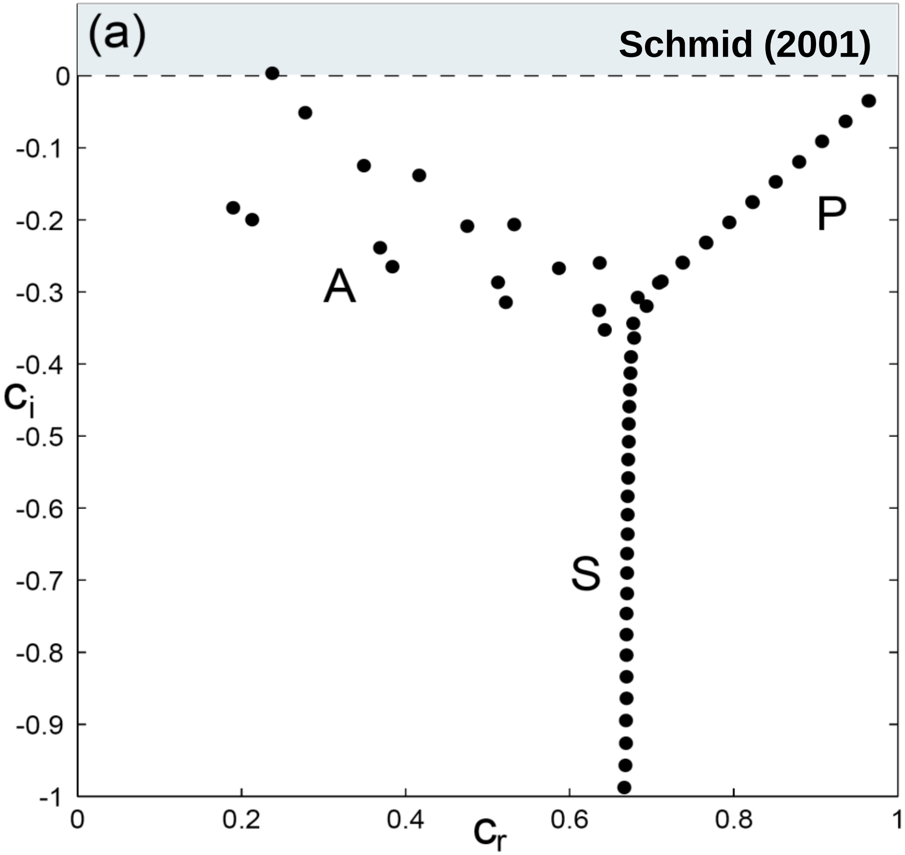

Spectrum for plane Poiseuille flow for $\alpha = 1, \beta = 0, Re = 10000$.

Orr mechanism (2D)

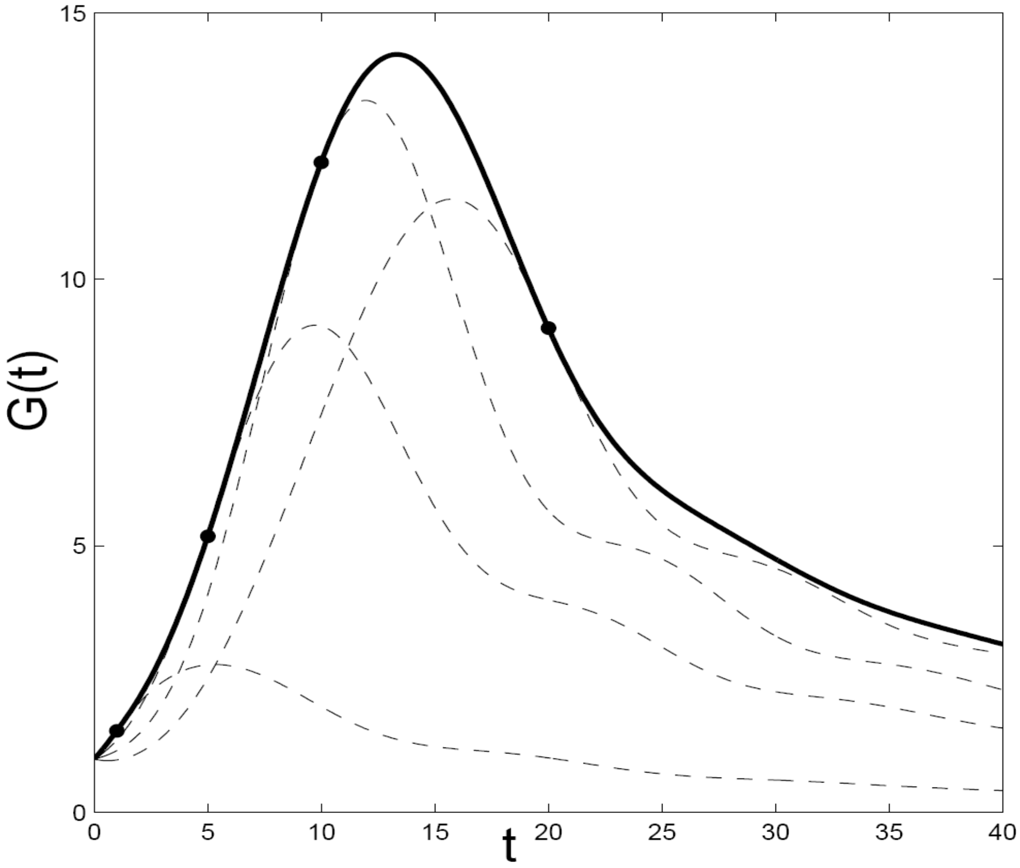

Amplification $G(t)$ for Poiseuille flow with $\mathrm{Re} = 1000, \alpha = 1$ (solid line)

« By-pass transition »

Trefethen et al (1993), Buttler & Farrell (1993) , Schmid & Henningson (2001)

Optimal perturbation (here in boundary layer)

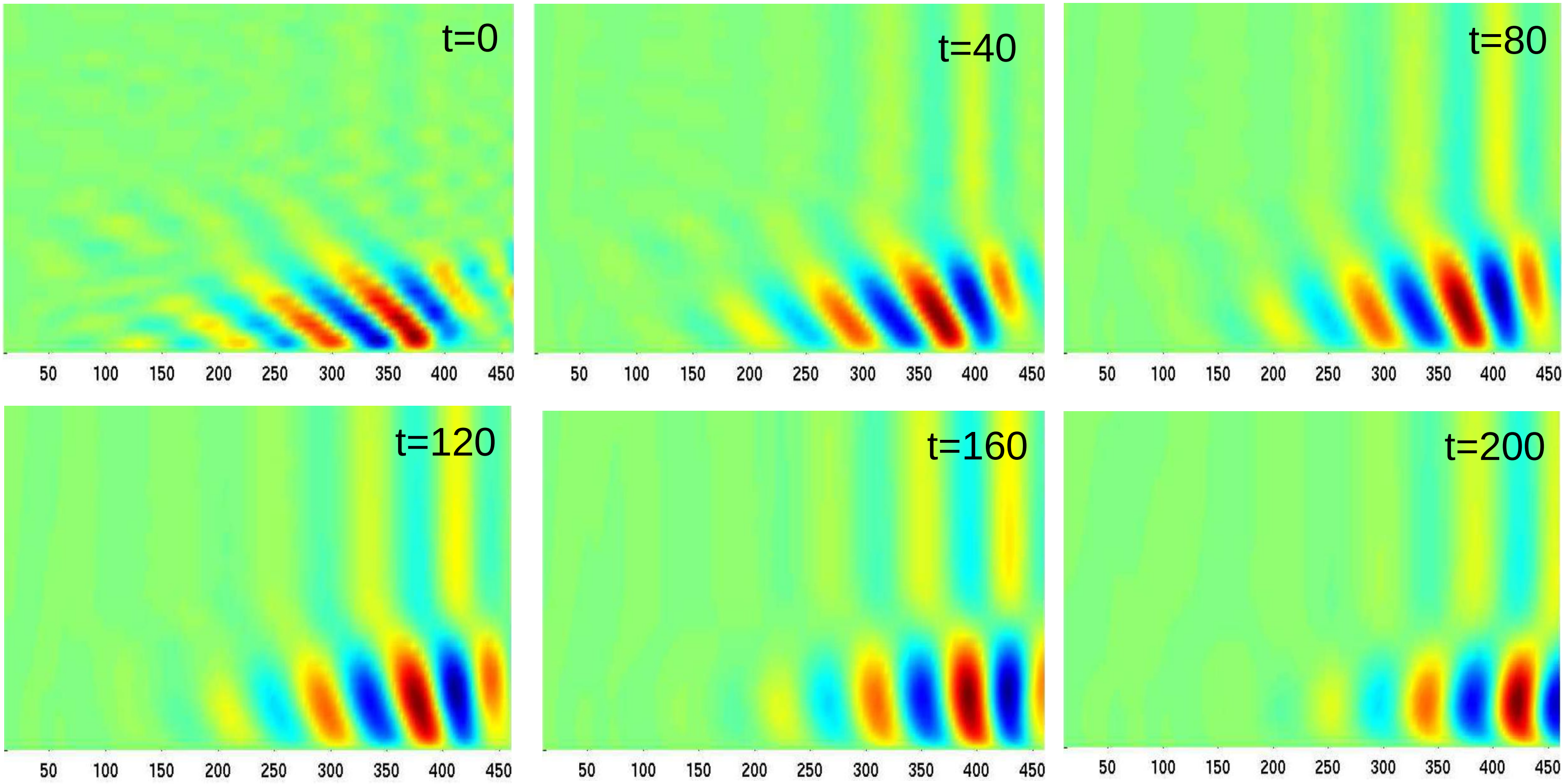

Orr mechanism

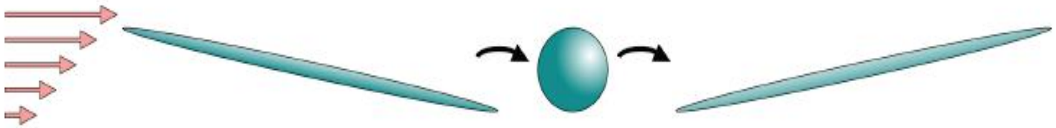

Plane Poiseuille flow
Lift-up mechanism (3D)

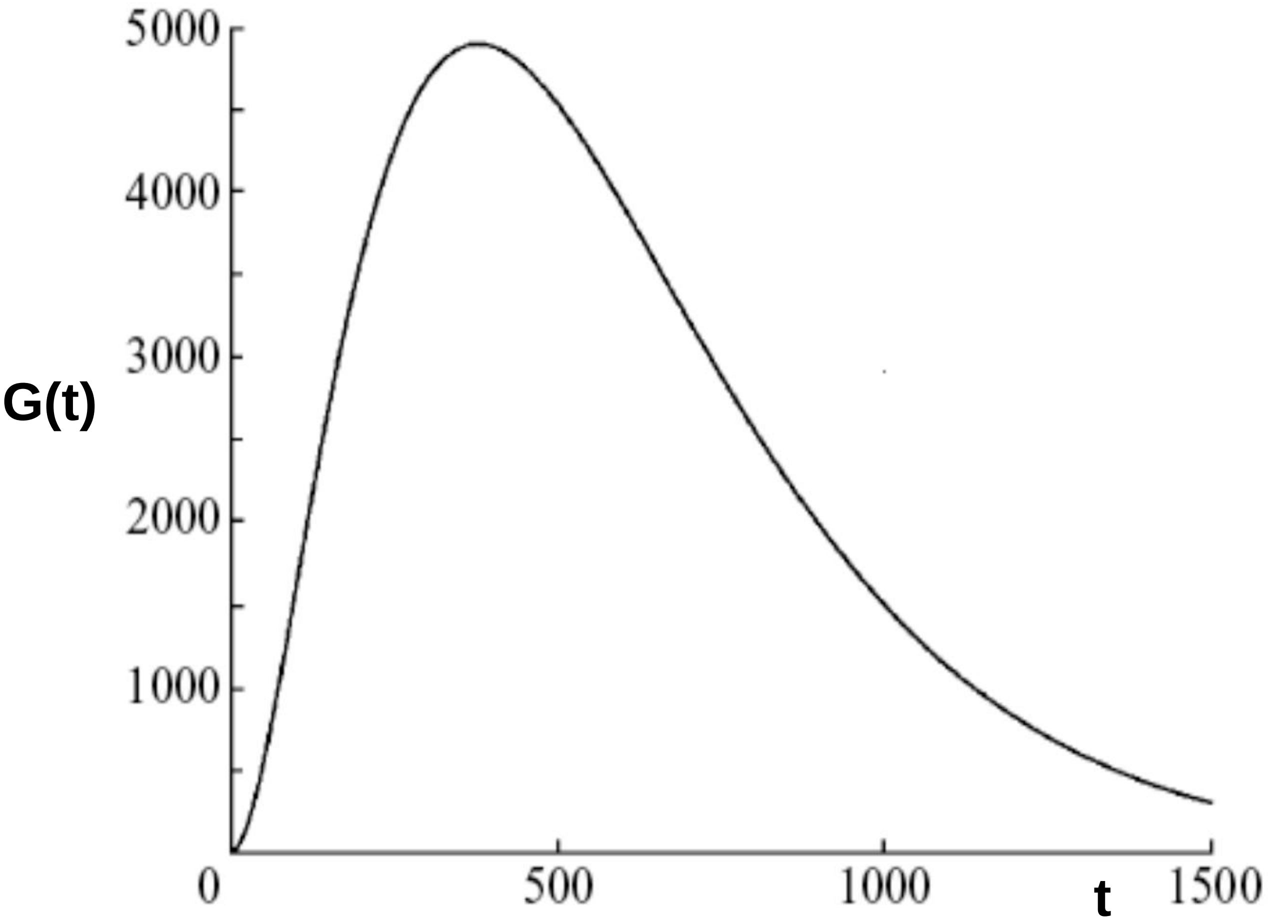

Re=5000, α=0, β=1

« By-pass transition »

Trefethen et al (1993), Buttler & Farrell (1993) , Schmid & Henningson (2001)

Lift-up mechanisms

Optimal transformation of vortices into streaks

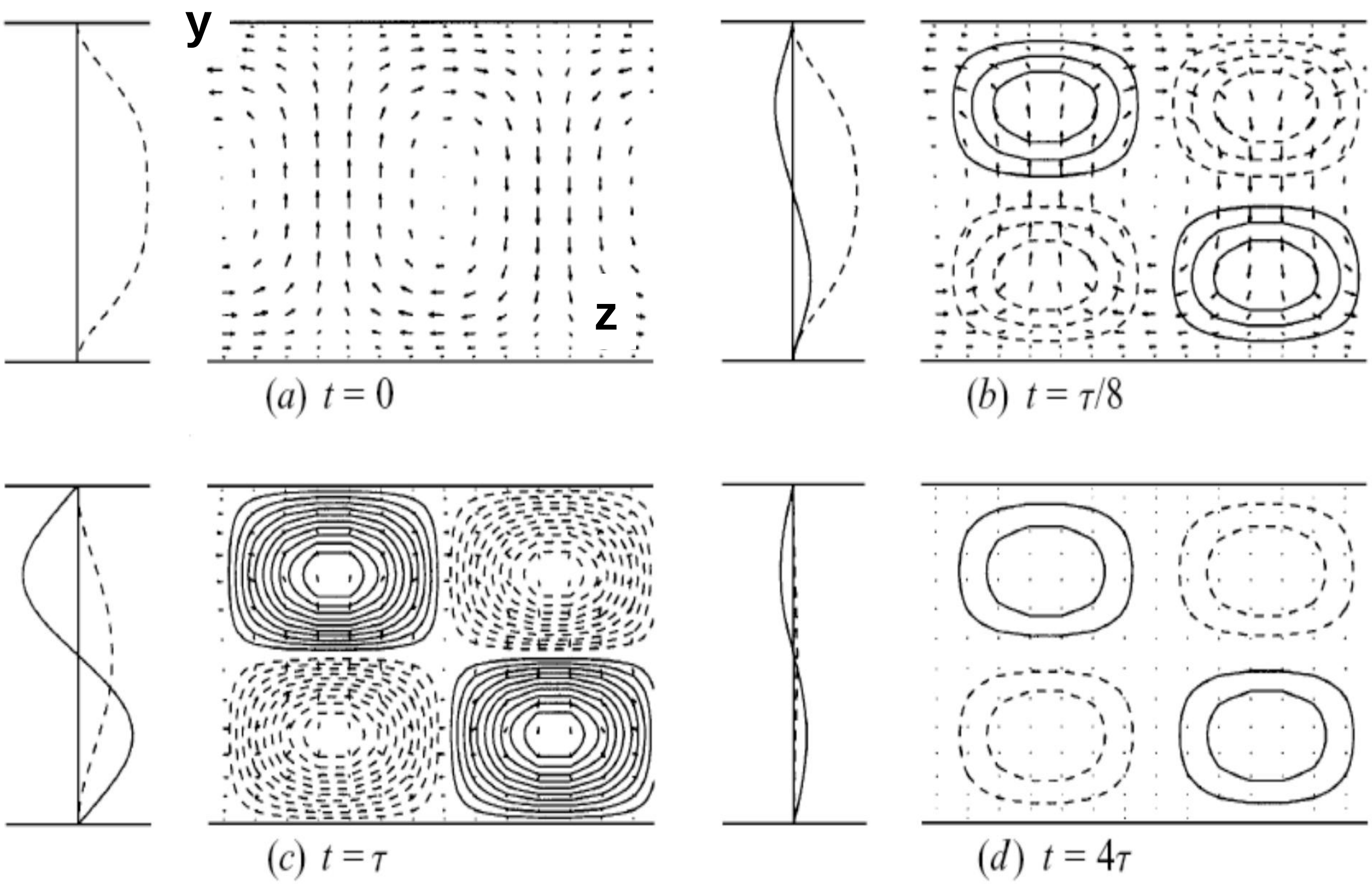

(a) $t = 0$

(b) $t = \tau/8$

(c) $t = \tau$

(d) $t = 4\tau$

Lift-up mechanism

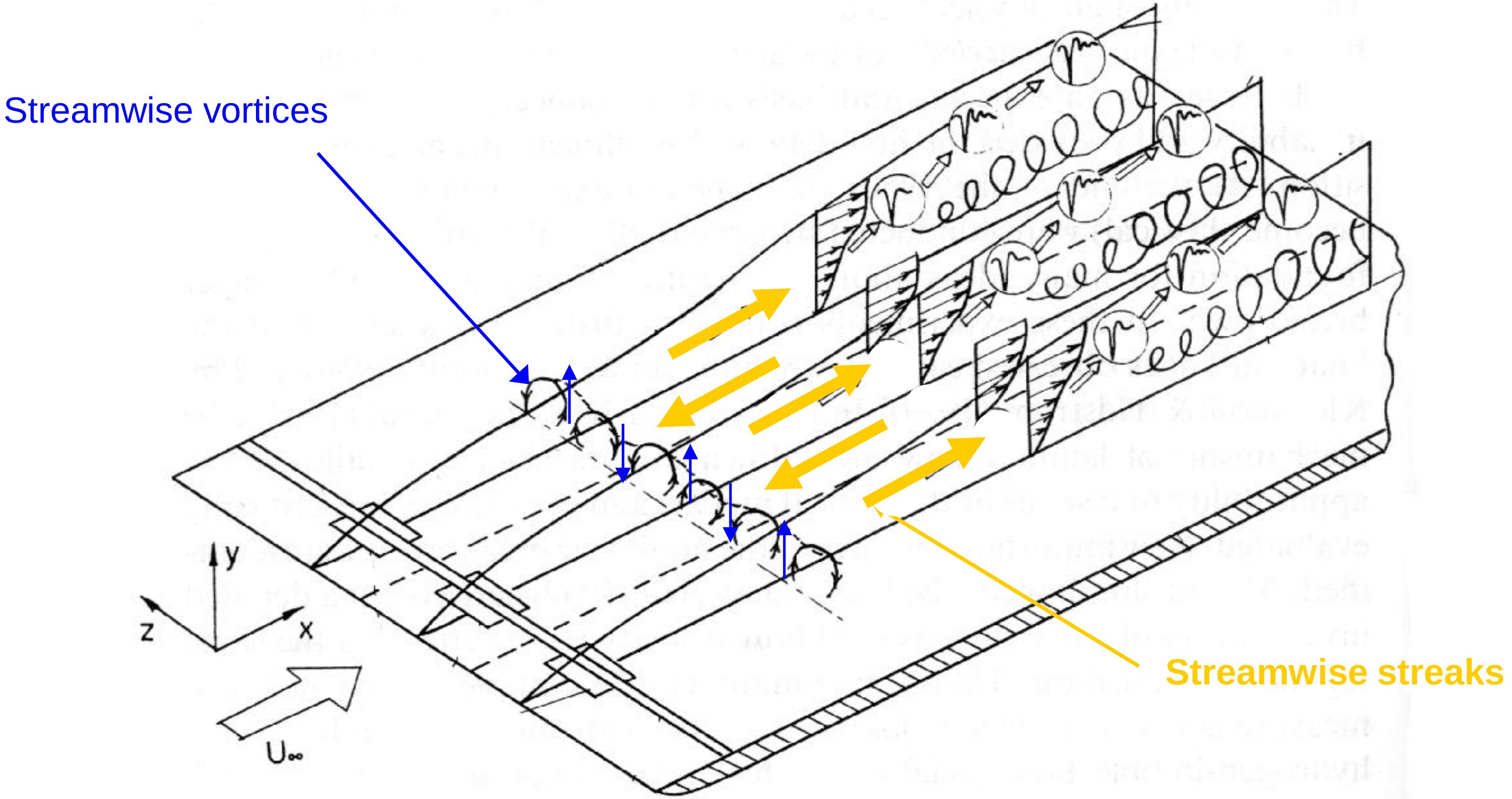

Schmid & Henningson.(2001)

Lift-up mechanism

Optimal transformation of vortices into streaks

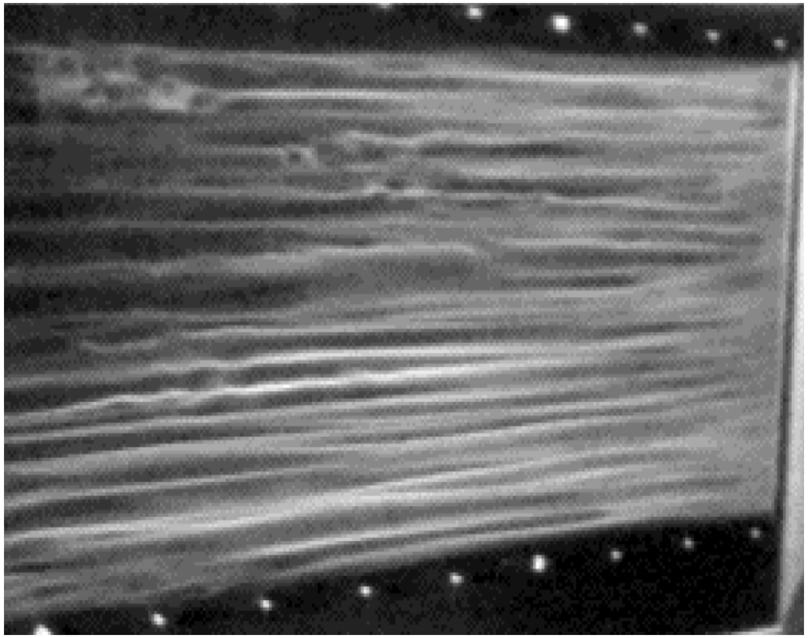

Alfredson & Matsubara (1996), streaky structures in the boudary layer

Isolines of maximum transient amplification $\beta=0$

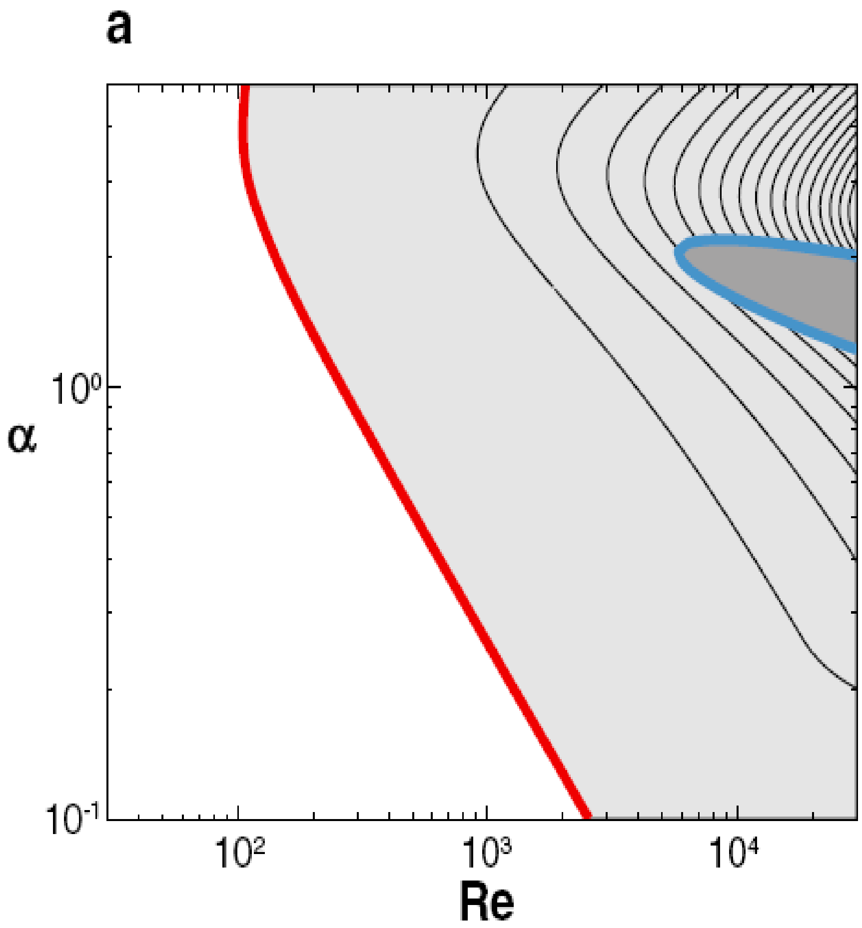

« By-pass transition »

Trefethen et al (1993), Buttler & Farrell (1993) , Schmid & Henningson (2001)

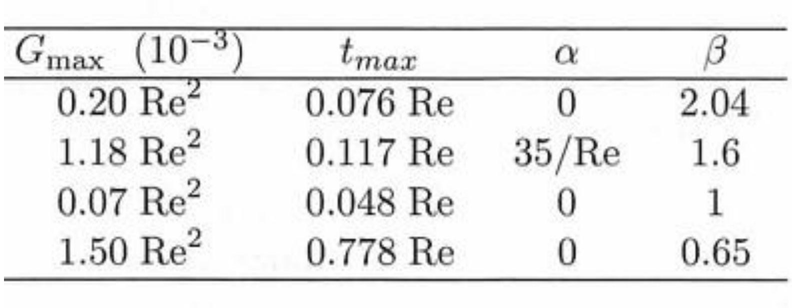

	$G_{\max}$ (10^{-3})	t_{max}	α	β
Plane Poiseuille	0.20 Re^2	0.076 Re	0	2.04
Couette	1.18 Re^2	0.117 Re	35/Re	1.6
Pipe	0.07 Re^2	0.048 Re	0	1
Boundary layer	1.50 Re^2	0.778 Re	0	0.65

Lift up mechanism in a square duct in the stable regime

Bye-pass transition to turbulence

fully developed turbulence

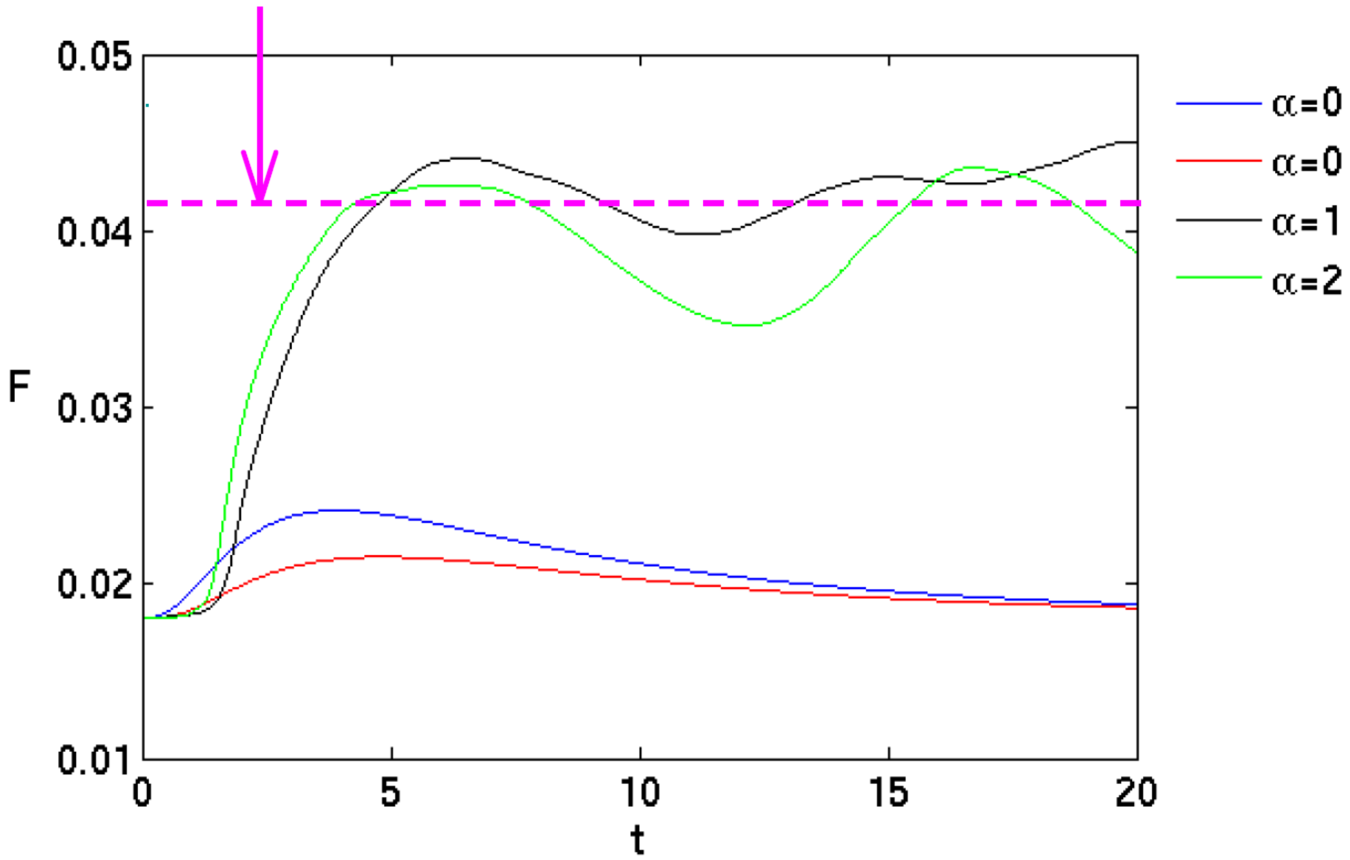

Bottaro et al. (2008)

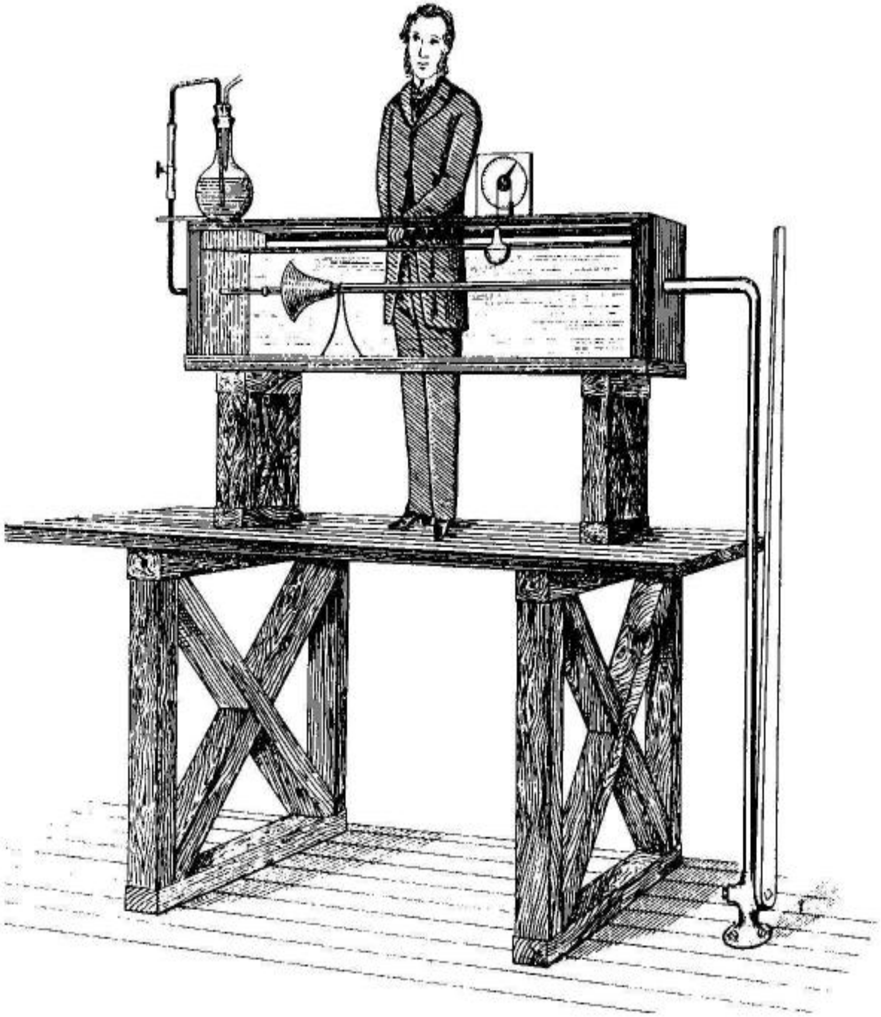

5.1 – *Osborne Reynolds en 1883 derrière son expérience à Manchester.*

Transition in Cylindrical Pipe Poiseuille flow

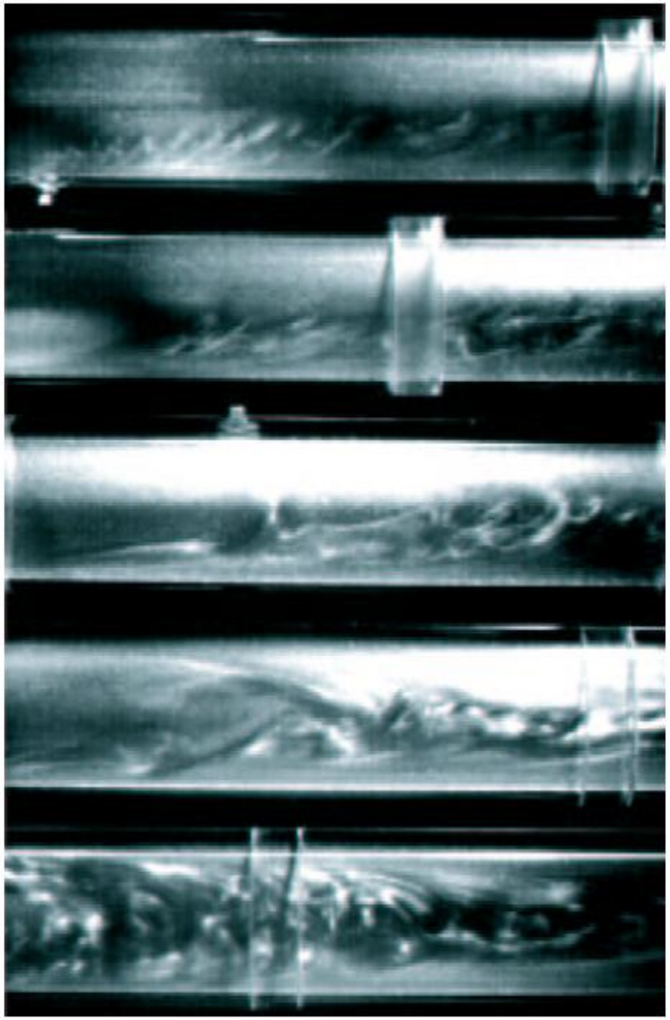

Mullin (2008)

Transition in Cylindrical Pipe Poiseuille flow

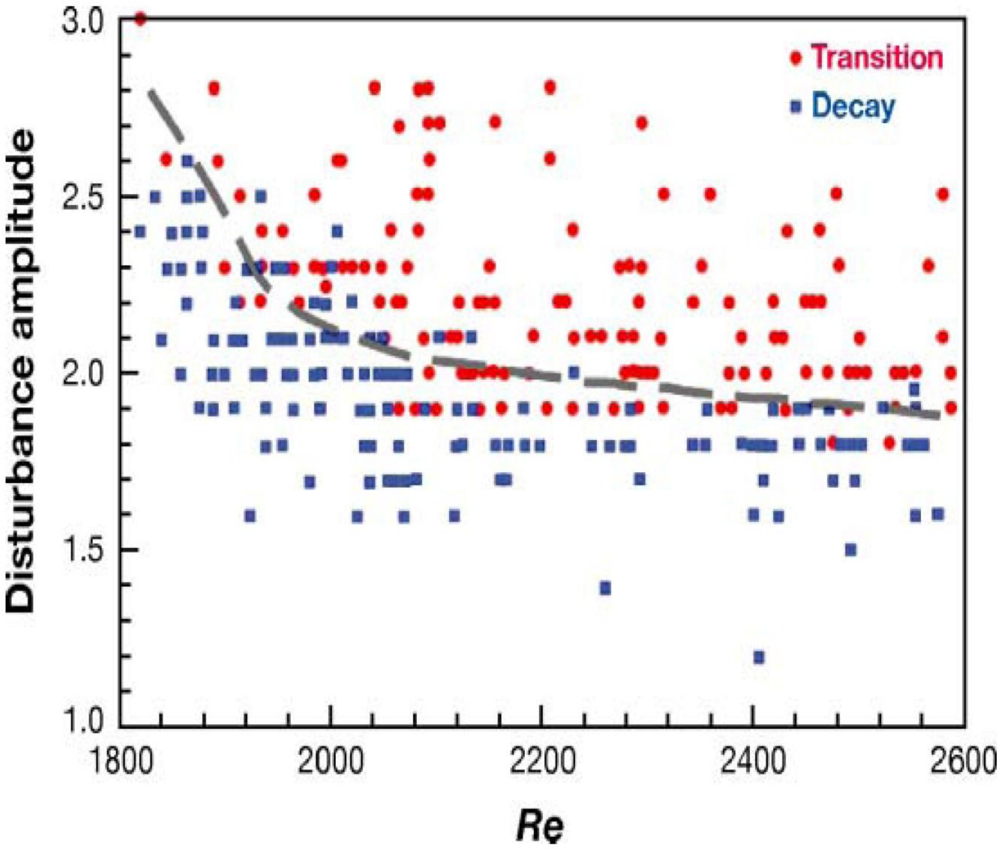

Mullin (2008)

Transition in Cylindrical Pipe Poiseuille flow

Numerical study

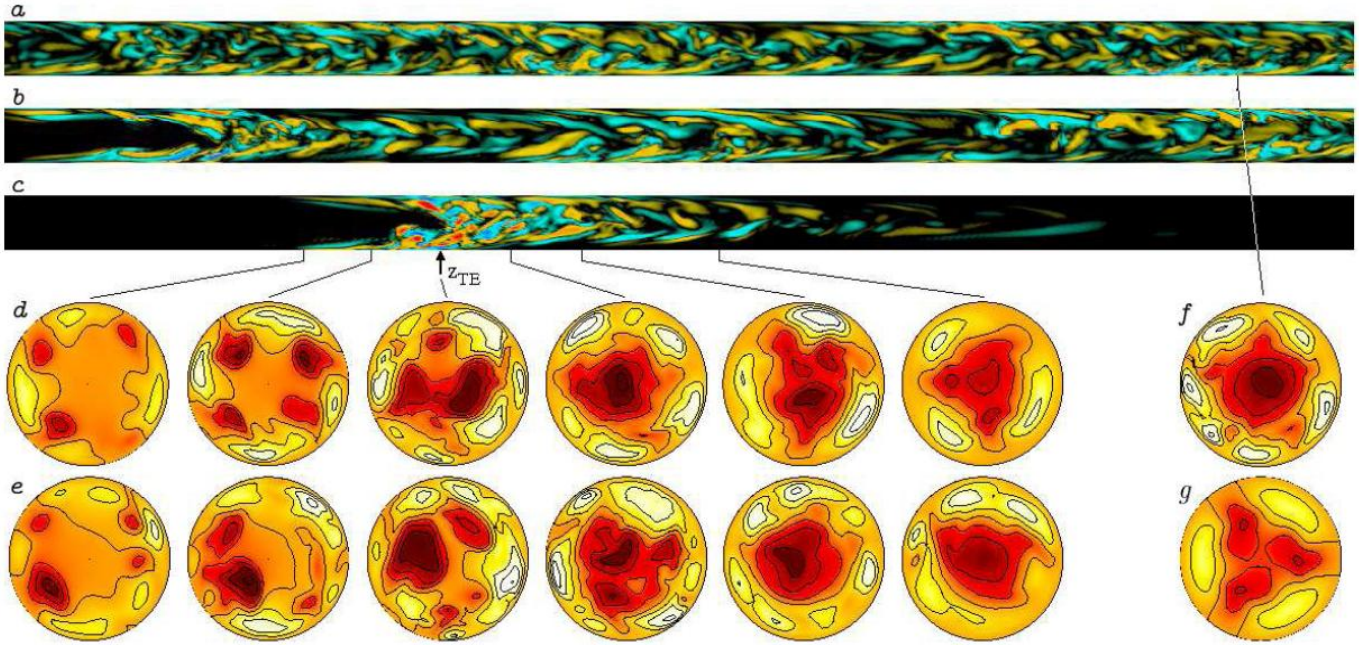

Kerswell (2008)

Tourbillon de Lamb-Oseen

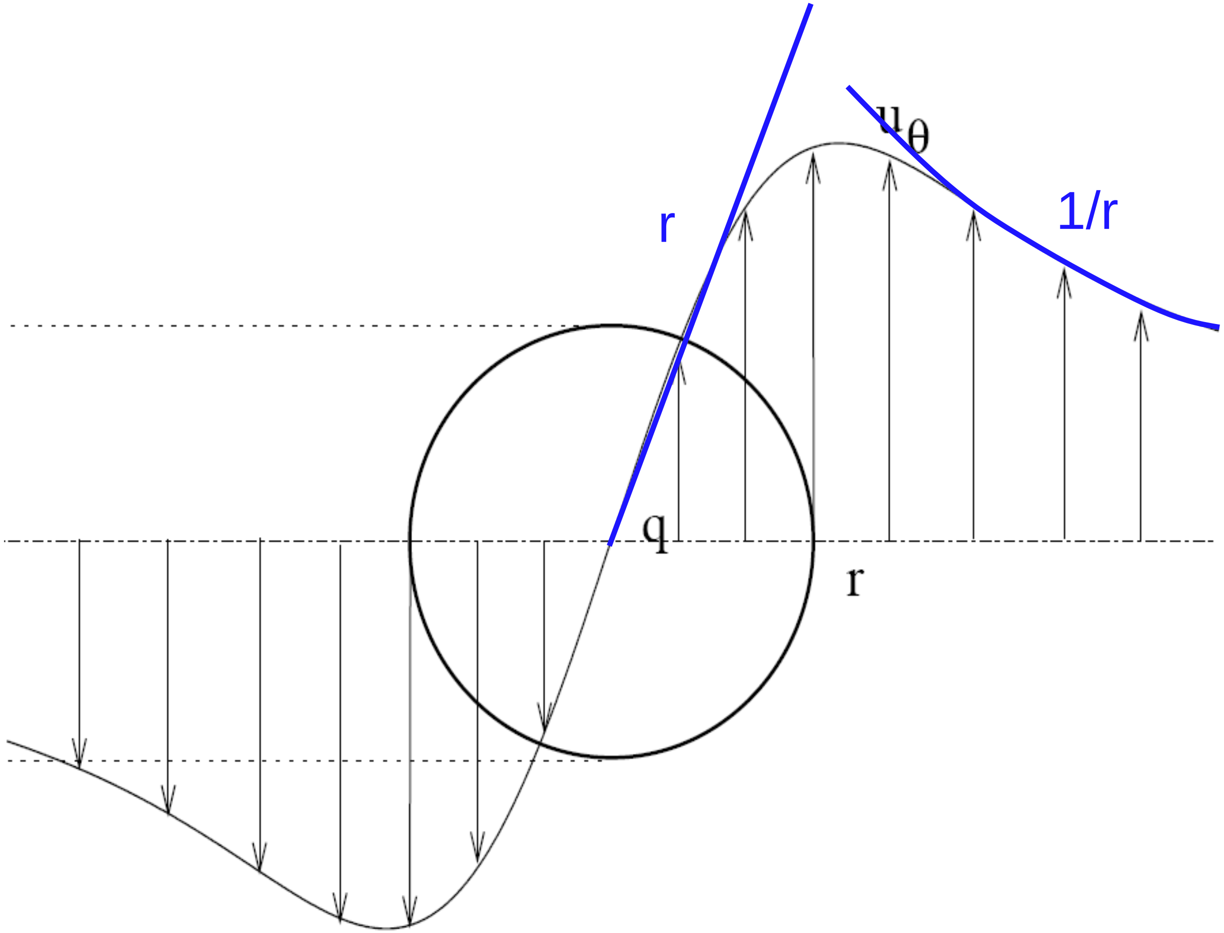

Stable lineairement!

Optimal growth m=1 as a function of axial wavenumber k and Re

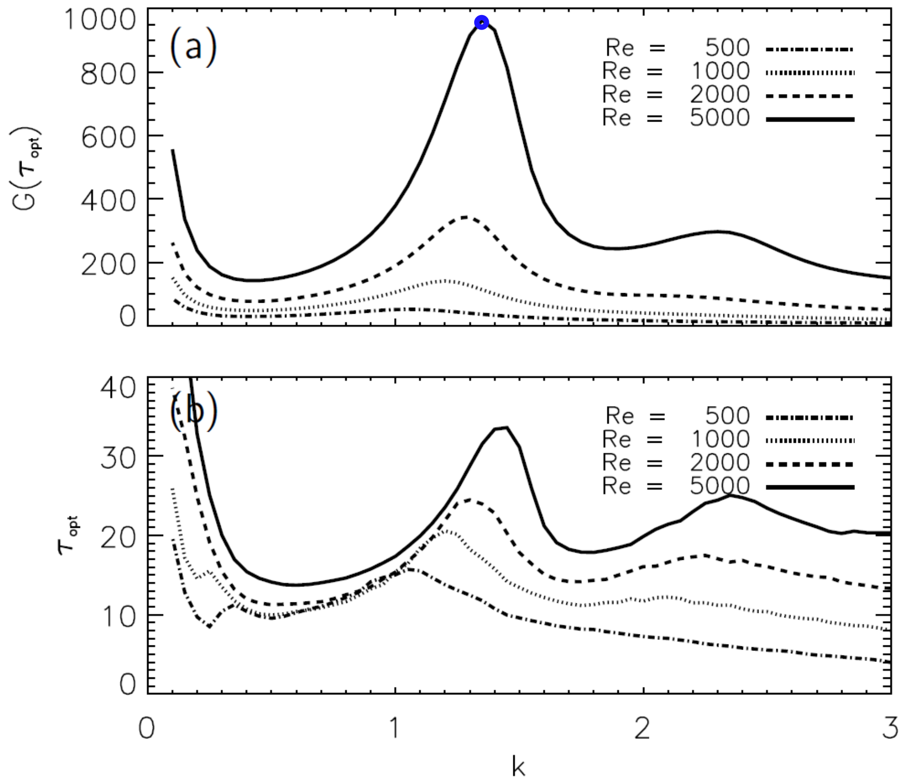

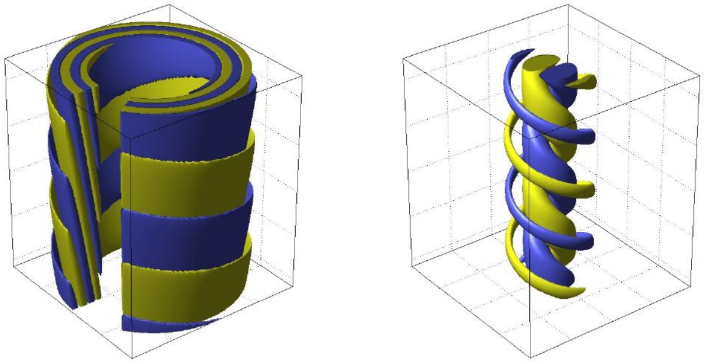

TOWARDS AN ELLIPTICAL STATE

Nonlinear evolution of the optimal perturbation with initial amplitude below a given threshold...

Re = 1000

TOWARDS AN ELLIPTICAL STATE

… and now ***ABOVE*** *the threshold*

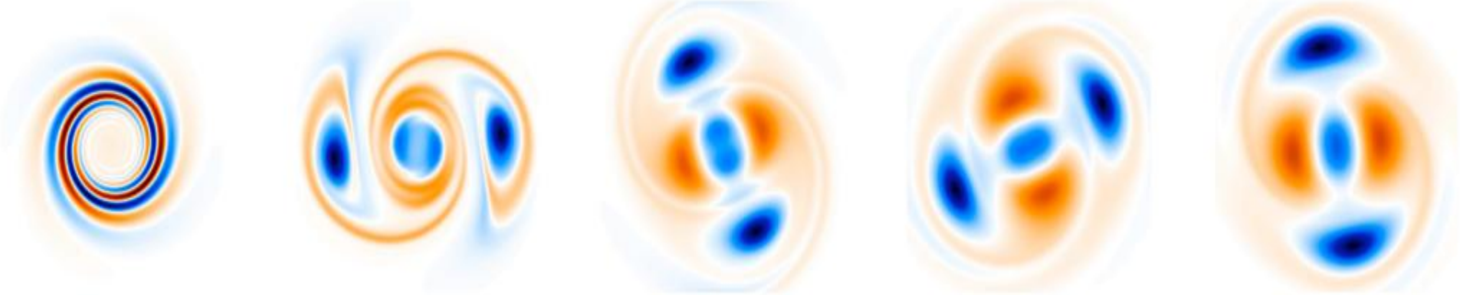

Re = 1000

TOWARDS AN ELLIPTICAL STATE

Reconstructed flow

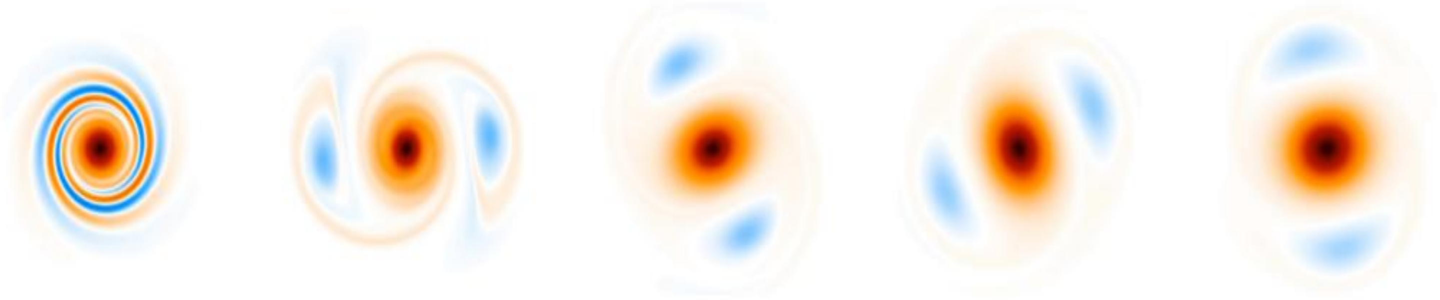

Re = 1000

Tripolar vortices?

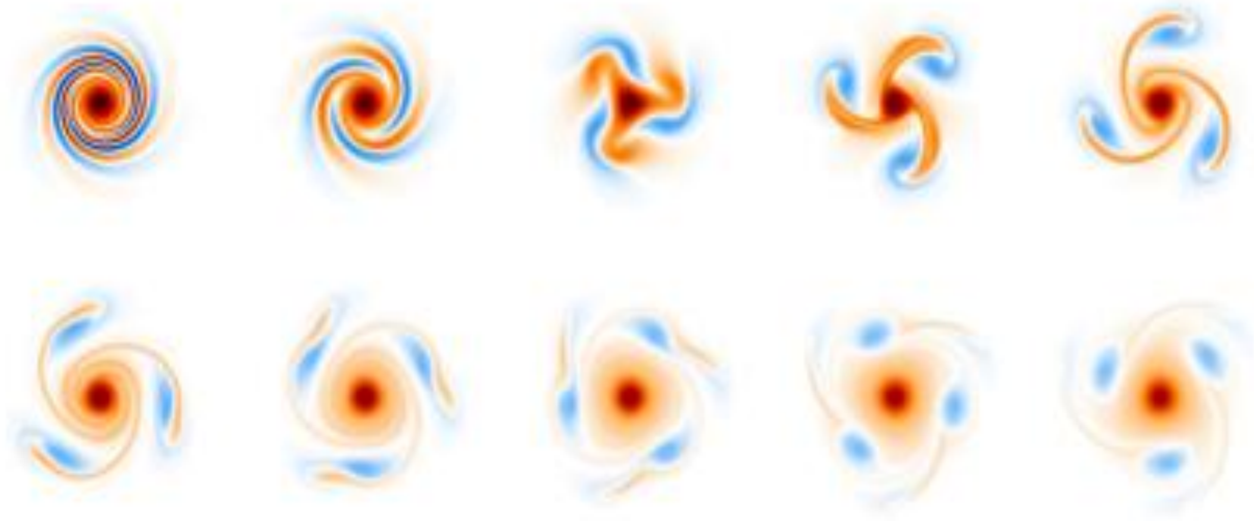

BASIN OF ATTRACTION'S SHRINKAGE

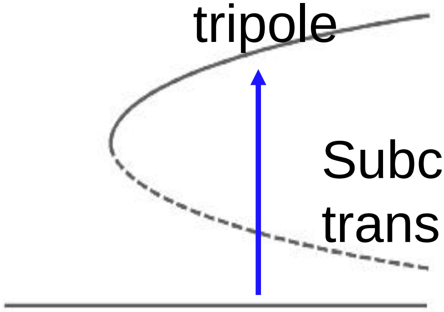

tripole

Subcritical transition

monople

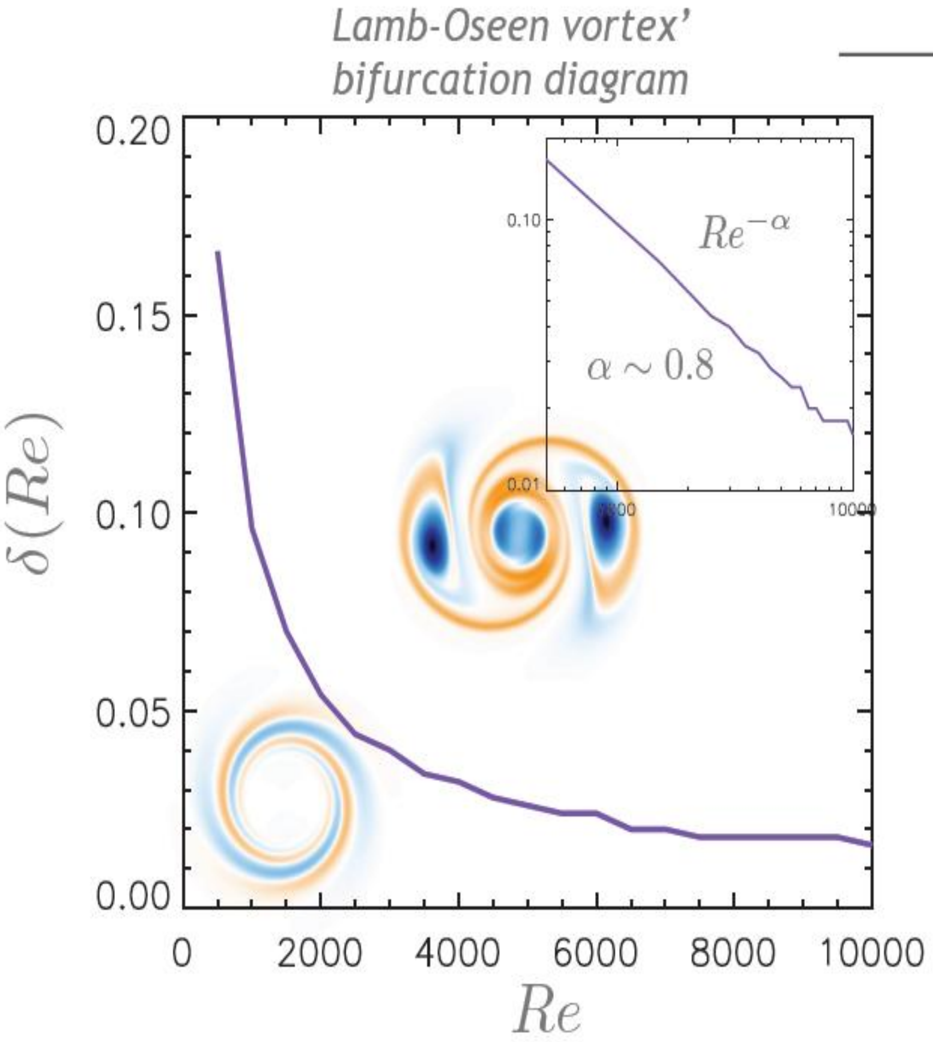

What about nonlinearities?

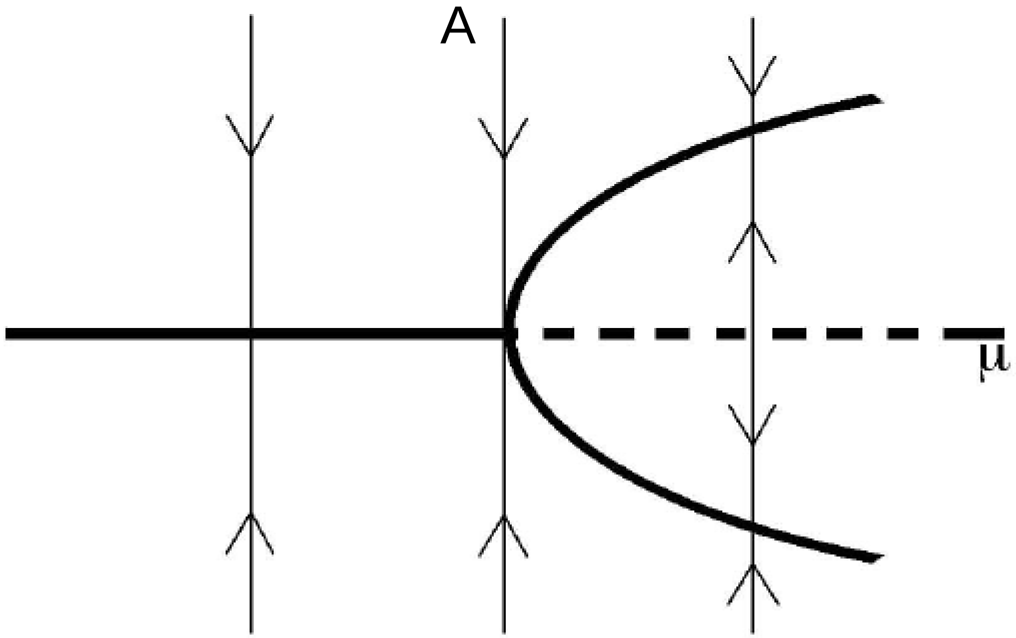

Supercritical fork bifurcation

What about nonlinearities?

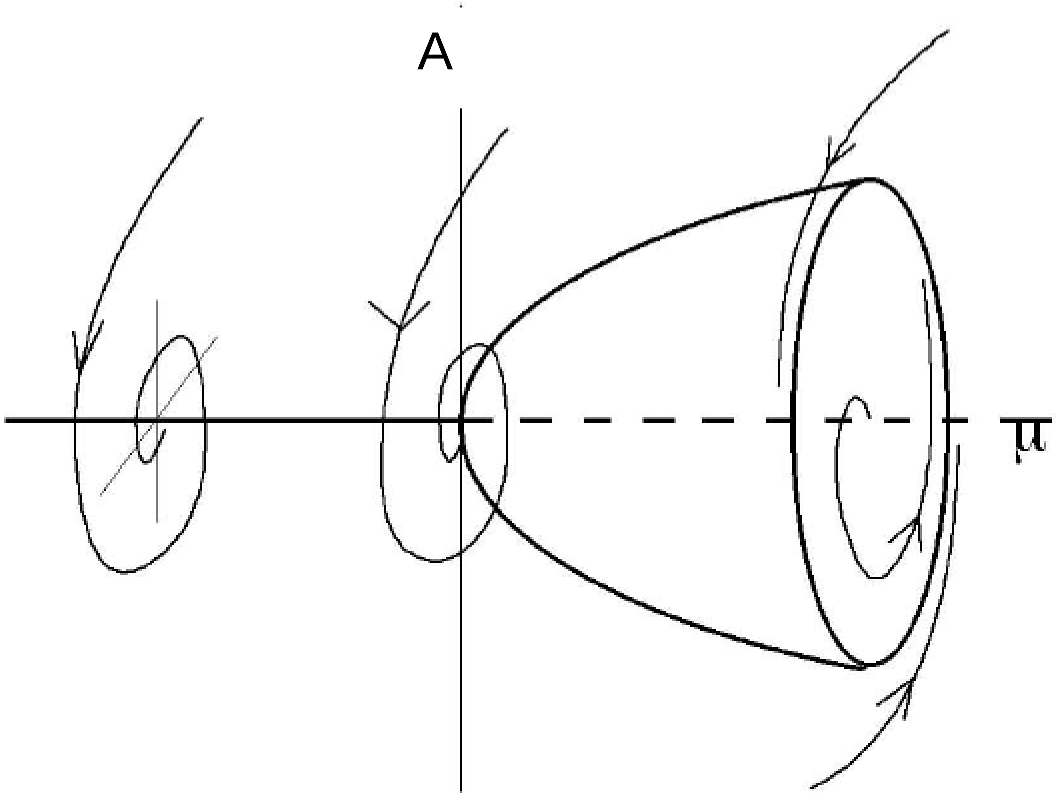

Hopf bifurcation

What about nonlinearities?

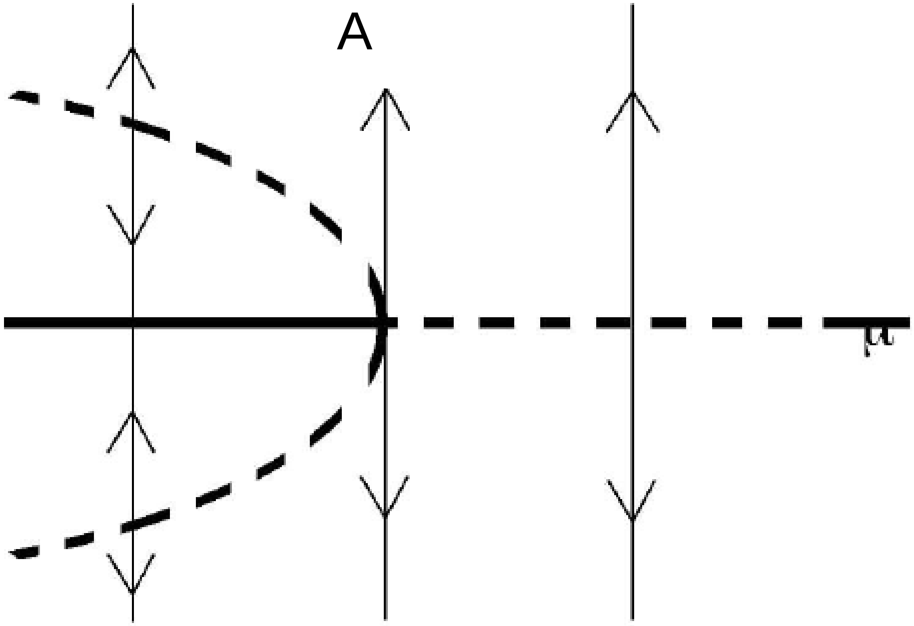

Subcritical fork bifurcation

What about nonlinearities?

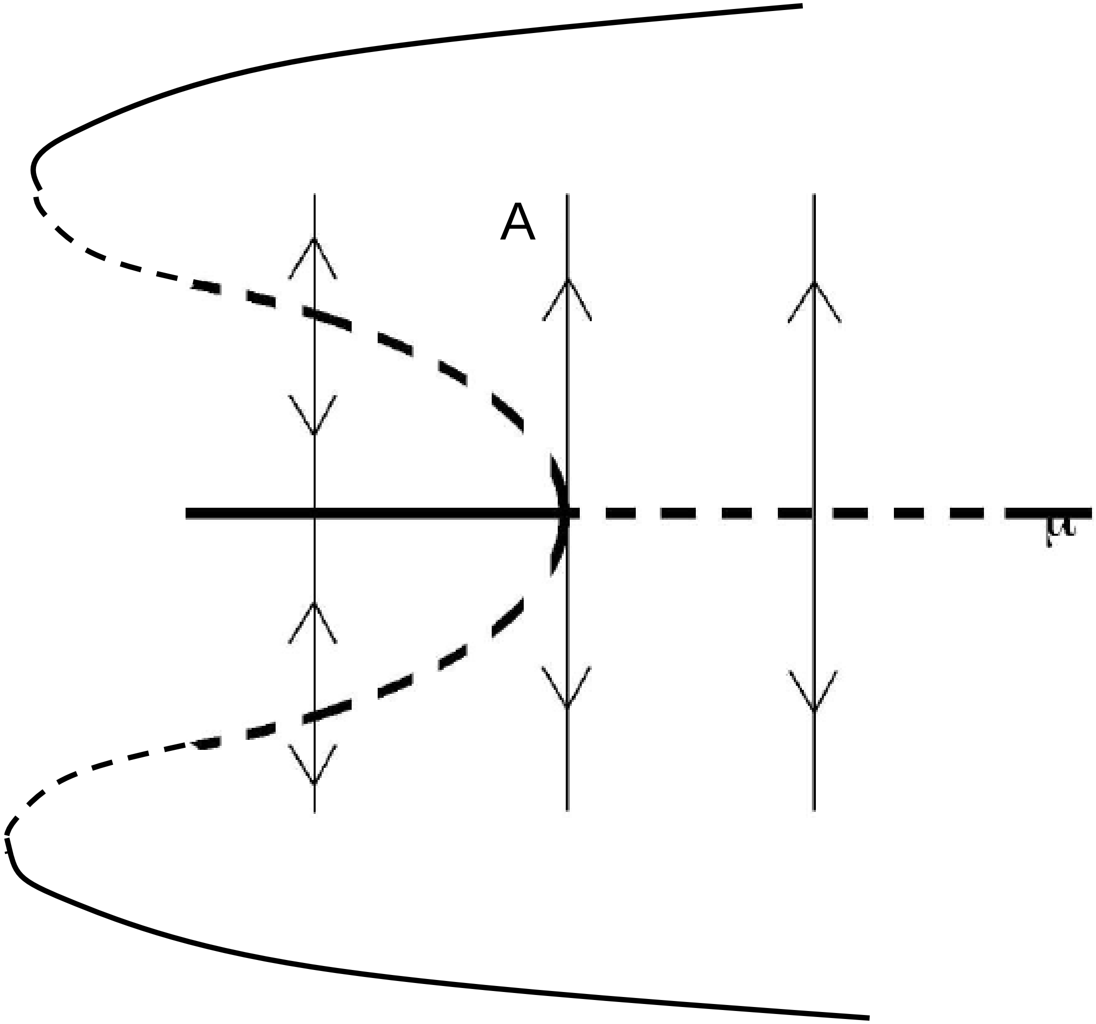

Subcritical bifurcation

What about nonlinearities?

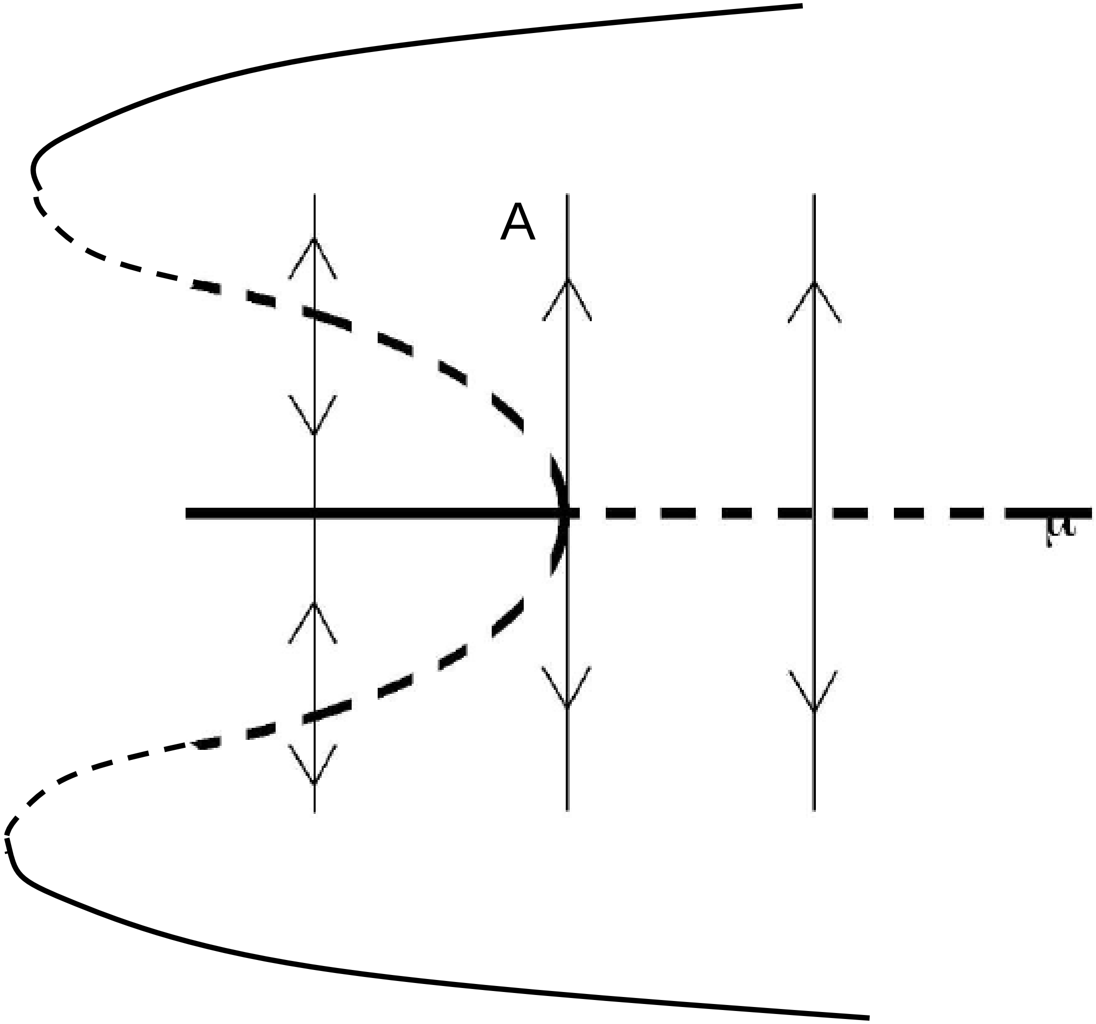

Hysteresis cycle!

What about nonlinearities?

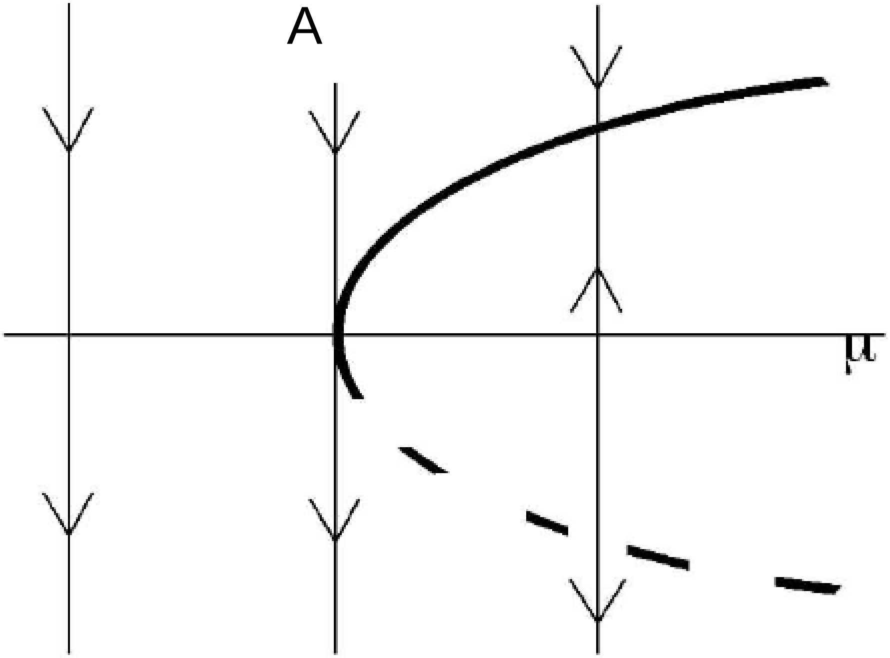

Saddle Node bifurcation

What about nonlinearities?

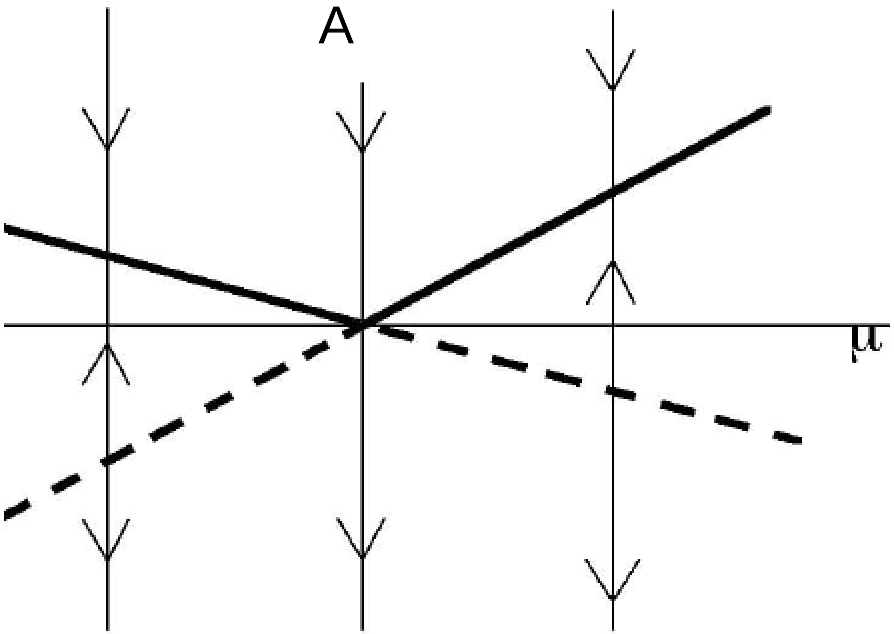

Transcritical bifurcation

Another example: asymmetric networks

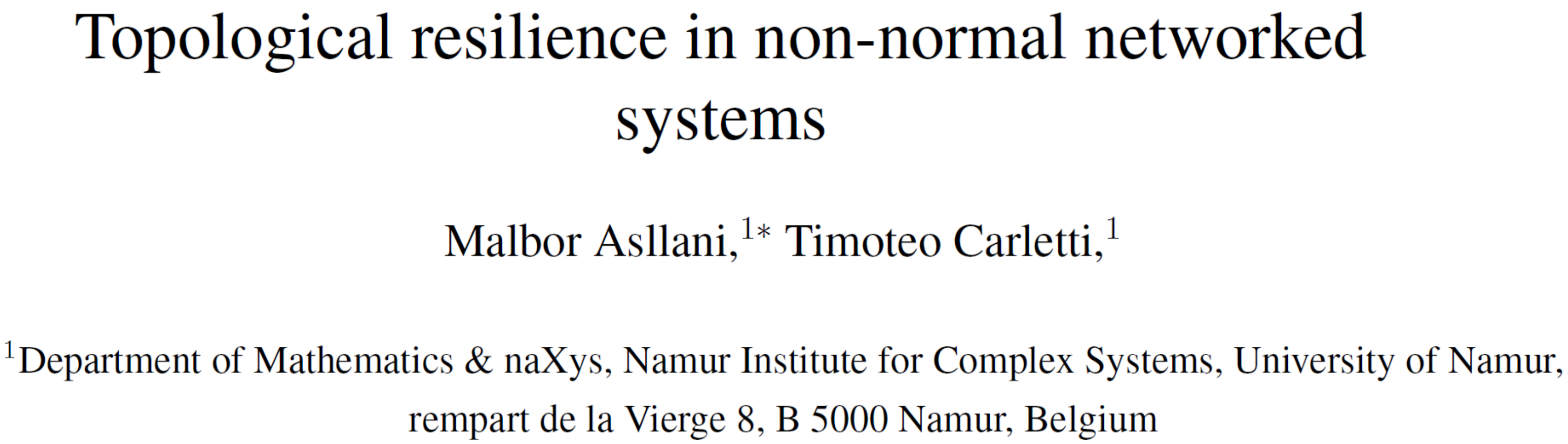

Topological resilience in non-normal networked systems

Malbor Asllani,[1]* Timoteo Carletti,[1]

[1]Department of Mathematics & naXys, Namur Institute for Complex Systems, University of Namur,
rempart de la Vierge 8, B 5000 Namur, Belgium

Another example: asymmetric networks

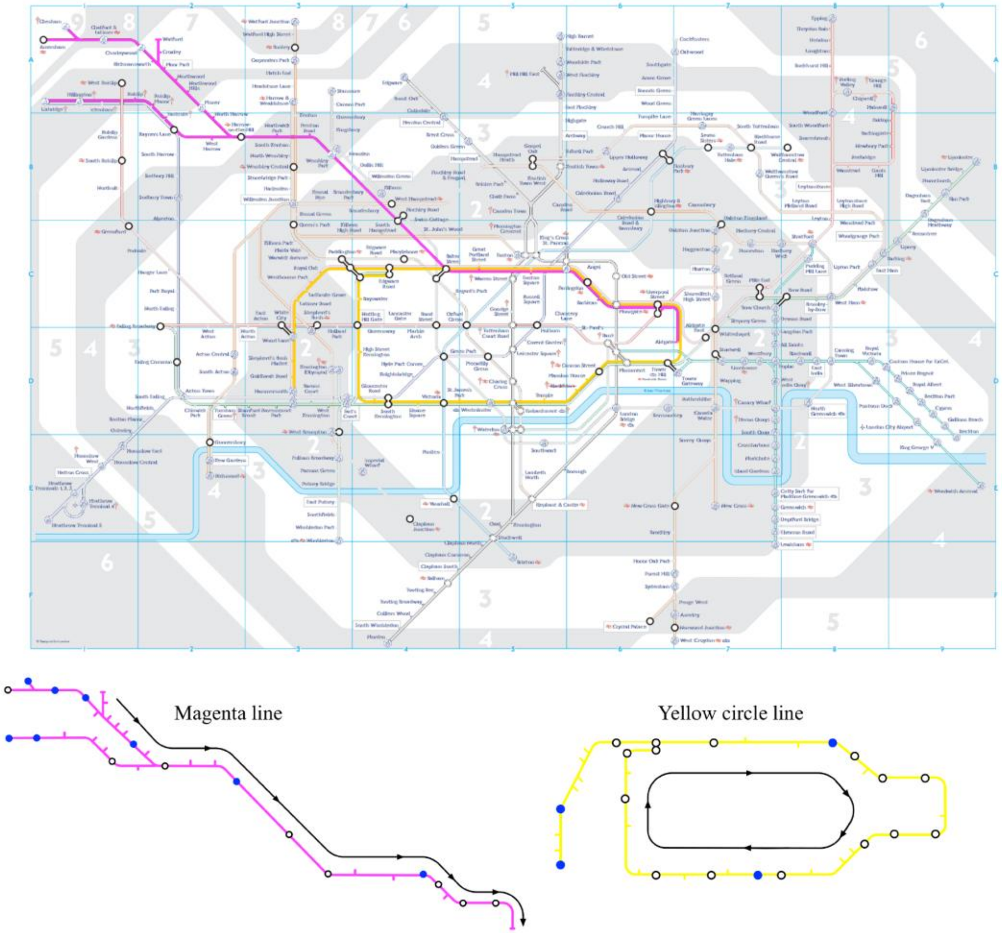

Figure 6: **The London Tube map**. Top panel: the whole London tube map where the yellow Circle Line and the magenta Metropolitan Line have been emphasized to show their different geographical emplacement and shape. In the bottom panels we separately present the Magenta line (left) and the Yellow line (right) and their respective flows of commuters.

Another example: asymmetric networks

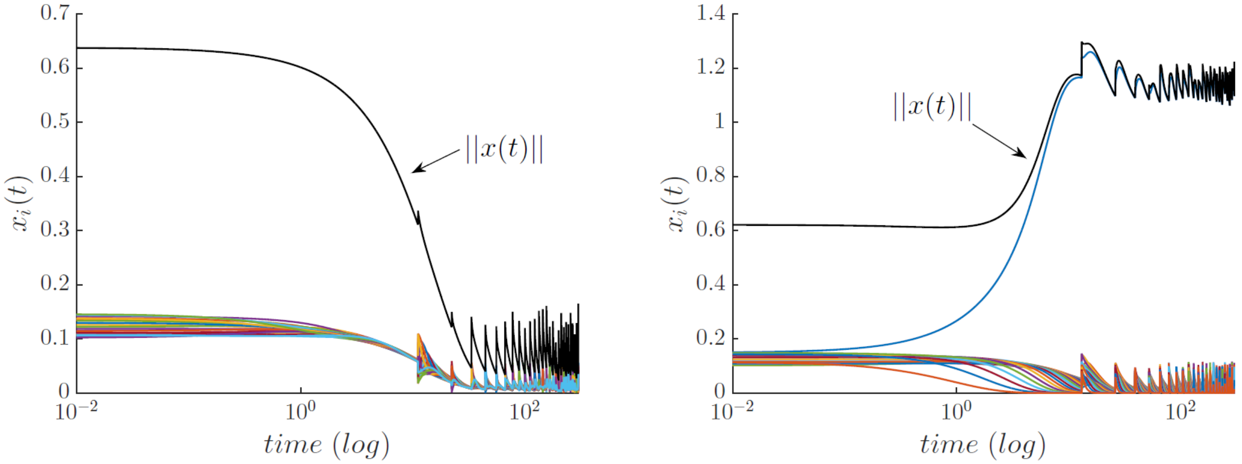

(a)

(b)

Figure 7: **Hypothetical Measles outbreak in the London Tube network.** Time evolution of the (normalized) number of infected individuals during the peak hours in the yellow Circle Line taking into account 27 stations (panel **(a)**) and in the magenta Metropolitan Line (panel **(b)**) considering 23 stations with the fluxes illustrated in Fig. 6. In the former case (panel **(a)**) we assumed the average number passengers to constant because in each station, the average number of passengers getting on equals that of those getting off. The circular topology and the Allee effect impede the outbreak of the epidemics. On the contrary, for the second case (panel **(b)**), we assume that, on average, as long the trains approach the downtown, the number of passengers increases, because most of the individuals have their destination in the city center. In this case, despite the presence of the Allee effect, the topology contributes to the outbreak of the measles epidemics once the train reaches the center. The parameters of the Allee model are $a = 1$, $A = 0.3$ and $D = 10$ for both cases.